sides of membranes lead to the vectorial transport of organic anions. These different transport characteristics may contribute to the effective function of the organic anion transport at both sides without any interference from each other.

URAT1: URAT1 (urate/anion exchanger) is expressed exclusively in the kidneys, where it is located in the apical membrane of proximal tubular cells (33). URAT1 exhibits Na^+-independent uptake of urate and regulates the serum urate level; genetic defects in URAT1 are the predominant causes of idiopathic renal hypouricemia. In a study using URAT1 cRNA-injected *Xenopus* oocytes, *cis*-inhibitory effects of uricosuric drugs (e.g., probenecid, benzbromarone, sulfinpyrazone, losartan) and *trans*-stimulatory effects of anti-uricosuric drugs (e.g., pyrazinoic acid, the metabolite of the antituberculous agent pyrazinamide) on the URAT1-mediated transport of urate were demonstrated (33).

3. Novel aspects of OATs

3.1. Novel transport substrates

Although about 10 years have passed since the discovery of OAT1, information regarding novel transport substrates of OAT family members is still increasing. The following substrates have been recently identified and well characterized in terms of OATs' roles in physiology and pathophysiology.

Neurotransmitter metabolites: Acidic metabolites of neurotransmitters derived from dopamine, epinephrine, norepinephrine, and serotonin have been suggested to be endogenous substrates of OAT3, the mRNA expression of which has been detected in the rat brain following its discovery in 1999 (14). Recently, we elucidated the expression of hOAT1 and hOAT3 in the choroid plexus of the human brain and their interactions with neurotransmitter metabolites using stable cell lines (34). Immunohistochemical analysis revealed that hOAT1 and hOAT3 are expressed in the cytoplasmic membrane and cytoplasm of the human choroid plexus. Neurotransmitter metabolites, namely, 5-methoxyindole-3-acetic acid (5-MI-3-AA), homovanillic acid (HVA), vanilmandelic acid (VMA), 3,4-dihydroxyphenylacetic acid (DOPAC), 5-hydroxyindole-3-acetic acid (5-HI-3-AA), *N*-acetyl-5-hydroxytryptamine (NA-5-HTT), melatonin, 5-methoxytryptamine (5-MTT), 3,4-dihidroxymandelic acid (DHMA), 5-hydroxytryptophol, and 5-methoxytryptophol (5-MTP) at 2 mM, inhibited PAH uptake mediated by hOAT1. On the other hand, melatonin, 5-MI-3-AA, NA-5-HTT, 5-MTT, 5-MTP, HVA, 5-HI-3-AA, VMA, DOPAC, 5-hydroxytryptophol, and methanephrine (MN) at 2 mM inhibited estrone sulfate uptake mediated by hOAT3. hOAT1 and hOAT3 mediated the transport of VMA but not that of HVA and melatonin. It is thought that hOAT1 and hOAT3 are involved in the efflux of various neurotransmitter metabolites from the cerebrospinal fluid to blood across the choroid plexus.

Although we could not observe HVA transport via hOAT3, Mori et al. revealed that rOat3 is the brain-to-blood HVA efflux transporter at the rat blood-brain barrier (BBB) (35). rOat3-expressing oocytes exhibited [^{3}H]HVA uptake ($K_m = 274\ \mu M$), which was inhibited by several organic anions, such as PAH, indoxyl sulfate, octanoic acid, and metabolites of monoamine neurotransmitters. Immunohistochemical analysis suggested that rOat3 is localized at the abluminal membrane of brain capillary endothelial cells. The results of Mori et al. provide the first evidence that rOat3 is expressed at the abluminal membrane of the rat BBB and is involved in the brain-to-blood transport of HVA. They suggested that this HVA efflux transport system is likely to play an important role in controlling the level of HVA in the central nervous system (CNS). Similar localization in brain capillary endothelial cells and uptake of [^{3}H]HVA in mouse Oat3 were reported by Ohtsuki et al. (36).

Bahn et al. demonstrated that OAT1 and OAT3 are involved in the secretion of bioactive tryptophan metabolites from the body (37). Tryptophan metabolites such as kynurenate (KYNA), xanthurenate (XA), and quinolinate are considered to be important for many physiological processes, especially brain function. Many of these metabolites are secreted with urine. Six tryptophan metabolites, including the bioactive substances KYNA, XA, and the serotonin metabolite 5-hydroxyindol acetate, inhibited [^{3}H]PAH or 6-carboxyfluorescein (6-CF) uptake by 50% – 85%, demonstrating that these compounds interact with Oat1 as well as with Oat3. The IC_{50} of KYNA for mOat1 was 34 μM and that for mOat3 was 8 μM, and the IC_{50} of XA for mOat1 was 15 μM and that for mOat3 was 11.5 μM. Quinolinate slightly but significantly inhibited [^{3}H]PAH uptake by mOat1 and had no effect on 6-CF uptake by mOat3. In the mouse brain, Oat1 was found to be expressed in neurons of the cortex cerebri and hippocampus as well as in the ependymal cell layer of the choroid plexus. Therefore, OAT1 and OAT3 are crucial for the regulation of CNS tryptophan metabolite concentration.

Antimetabolites: Thiopurines are used as antileukemic drugs. During chemotherapy CNS relapses occur due to the proliferation of leukemic cells in the CNS resulting from restricted drug distribution in the brain. The molecular mechanism for this limited cerebral distribution remains unclear. Mori et al. reported that rOat3 is involved in the brain-to-blood transport of thiopurines at the BBB and is one of the mechanisms of limited

cerebral distribution (38). rOat1 and rOat3 exhibited [^{14}C]6-MP uptake (K_m = 98 μM for rOat1, 50.5 μM for rOat3). rOAT3-mediated [^{14}C]6-MP uptake was also inhibited by other thiopurine derivatives. Although methotrexate inhibited rOAT3-mediated [^{14}C]6-MP uptake, the K_i value was 17.5-fold greater than the estimated brain concentration of methotrexate in patients receiving chemotherapy. Accordingly, 6-MP would undergo efflux transport by OAT3 from the brain without any inhibitory effect from coadministered methotrexate in chemotherapy. The results of Mori et al. may provide a molecular basis for improving the permeability of thiopurine nucleobase analogs to the brain and offer an approach to reduce CNS relapses during treatment of patients with ALL. The identification of 6-MP and another antimetabolite, 5-fluorouracil (5-FU), as novel transport substrates for mOat3 was also reported by Kobayashi et al. (39). K_m for 6-MP was 4.01 μM and that for 5-FU was 53.9 nM.

AMPA receptor antagonist: Zonampanel monohydrate (YM872; [2,3-dioxo-7-(1*H*-imidazol-1-yl)-6-nitro-1,2,3,4-tetrahydro-1-quinoxalinyl]acetic acid monohydrate) is a novel α-amino-3-hydroxy-5-methylisoxazole-4-propionic acid (AMPA) receptor antagonist. The major elimination route for zonampanel is by urine via the kidneys. Hashimoto et al. elucidated the molecular mechanism of the renal excretion of zonampanel using cells stably expressing hOAT1, hOAT2, hOAT3, and OAT4 as well as human organic cation transporter (hOCT) 1 and hOCT2 (40). A time- and concentration-dependent increase in [^{14}C]zonampanel uptake was observed in cells expressing hOAT1, hOAT3, and OAT4. Kms for hOAT1, hOAT3, and OAT4 were 1.4, 7.7, and 215 μM, respectively. These results suggest that the efficient urinary excretion of zonampanel is due to the renal tubular secretion mediated by the organic anion transporters hOAT1, hOAT3, and OAT4.

Xanthine-related compounds: Caffeine (1,3,7-trimethylxanthine, 1,3,7-TMX) is daily and widely consumed in beverages and food and is mainly metabolized to paraxanthine (1,7-dimethylxanthine, 1,7-DMX) and 1-methylxanthine (1-MX). One-third of 1-MX is excreted unchanged into urine, and the remainder undergoes hydroxylation to 1-methyluric acid. Rengelshausen et al. investigated the effect of caffeine and its main metabolites on hOAT1 using Chinese hamster ovary (CHO) cells overexpressing hOAT1 (41). The uptake of 6-CF into CHO-hOAT1 cells was significantly inhibited by 1-MX (100 μM). 1-MX (500 μM) was equieffective to 100 μM probenecid. In contrast, caffeine and 1,7-DMX did not inhibit the transport of 6-CF at concentrations up to 500 μM. Thus, the caffeine metabolite 1-MX inhibits the transport activity of hOAT1 in vitro. Because of the wide consumption of caffeine, an inhibitory effect of its metabolite 1-MX on renal tubular secretion mediated by hOAT1 might contribute to the pharmacokinetic variability of drugs such as methotrexate.

Sugawara et al. further examined the inhibitory effects of xanthine- and uric acid-related compounds on the transport of PAH using CHO-K1 cells stably expressing hOAT1 from the aspect of the structure-affinity relationship (42). The order of potency for the inhibitory effects of xanthine-related compounds on PAH uptake was 1-methyl derivative > 7-methyl derivative > 3-methyl derivative = xanthine > 1,3,7-trimethyl derivative (caffeine). The order of potency of the inhibition was 1,3,7-trimethyluric acid > 1,3-dimethyluric acid > 1,7-dimethyluric acid > 1-methyluric acid > uric acid. A significant correlation between inhibitory potency and lipophilicity of the tested uric acid-related compounds was observed. The main determinant of the affinity of xanthine-related compounds is the position of the methyl group. On the other hand, lipophilicity is the main determinant of the affinity of uric acid-related compounds.

HMG-CoA reductase inhibitor: It was recently demonstrated that pravastatin is a relatively specific inhibitor of rOat3 rather than rOat1 (43). Pravastatin, a structural analog of 3-hydroxy-3-methylglutaryl-coenzyme A (HMG-CoA), is a competitive inhibitor of HMG-CoA reductase and therefore blocks the synthesis of cholesterol in the liver. We have elucidated the interactions of human and rat organic anion transporters (hOATs and rOats) with pravastatin (44). Pravastatin inhibited hOAT1/rOat1, hOAT2/rOat2, hOAT3/rOat3, and OAT4. The mode of inhibition was noncompetitive for hOAT1 and hOAT2, whereas it was competitive for hOAT3 and hOAT4. The effects of OAT inhibitors on OAT1, OAT2, and OAT3 exhibited some but not so remarkable interspecies differences between humans and rats. These results would be useful for the extrapolation of results of the functional analysis of rat organic anion ransport using OAT inhibitors in humans.

Nicotinate: Recently, we demonstrated nicotinate transport via URAT1 in a *Xenopus* oocyte system (33). Nicotinate has been used as a lipid-lowering agent producing beneficial changes in serum lipids for atherosclerosis regression. Although inhibitory effects of nicotinate on the synthesis and secretion of VLDL in the liver have been reported, its hepatic transport mechanism was still unknown. We examined, by using cells stably expressing hOAT2, the possibility that hepatic OAT isoform OAT2 functions as an entrance pathway for nicotinate in the liver (45). hOAT2 mediated a time- and concentration-dependent uptake of

nicotinate. hOAT2-mediated nicotinate uptake showed structural specificity and was inhibited by some organic anions such as ICG, glibenclamide, and probenecid and by some NSAIDs (salicylic acid, diclofenac, ketoprofen, indomethacine, and ibuprofen). Identification of the hepatic nicotinate transporter will contribute to the understanding of the molecular basis of drug-drug interactions such a as salicylate-induced increase in serum nicotinate level.

3.2. Novel OAT isoforms

Oat5: Oat5 was recently identified from the mouse (46) and rat (47). It is expressed exclusively in the kidneys, and rat Oat5 is localized at the apical side of the late segment of proximal tubules (47). Oat5 mediates the transport of steroid sulfates as well as ochratoxin A. Mouse Oat5 (46) and rat Oat5 (47) are functional and not identical to non-functional human OAT5 reported by Sun et al. (48). The most surprising finding of our study is that rOat5 interacted not only with the five-carbon dicarboxylate α-ketoglutarate (C5) but also with the four-carbon dicarboxylate succinate (C4), which has not been reported as a counterion for the classical renal organic anion transport system to mediate organic anion/succinate exchange (47). In contrast, the basolateral OAT isoform OAT3 did not exhibit the interaction to succinate. These findings indicate that rOat5 is the renal organic anion transporter that may mainly function as an apical pathway for the reabsorption of some organic anions driven by an outward gradient of both α-ketoglutarate and succinate. It seems appropriate that the apical isoforms of OAT utilize C4 succinate as a counterion, whereas the basolateral OATs utilize C5 α-ketoglutarate as a counterion, to separate the transport of organic anions at both sides of proximal tubular cells (Fig. 2). This idea is supported by results showing that the apical membrane isoform OAT4-mediated transport was inhibited by succinate as well as glutarate (P. Jutabha, et al., unpublished observation). Interestingly, urate transport via the urate/anion exchanger (URAT1) localized at the renal apical membrane was also inhibited by succinate at a millimolar concentration in the *Xenopus* oocyte system (33). It is thought that succinate exchange in addition to α-ketoglutarate exchange is a common mechanism for the apical membrane isoforms of OAT family members.

Oat6: This putative organic anion transporter was recently isolated (49). Oat6 is expressed predominantly in the mouse olfactory mucosa but not in the kidneys or brain. Oat6 expression is also observed in the testes. The genomic localization of Oat6 is proximal to the Oat1/Oat3 gene pair. Based on sequence homologies, this protein was designated Oat6. However, further studies are needed to determine its substrate specificity and therefore its involvement in the transport of organic anions.

OAT7: We identified a novel organic anion transporter, OAT7, exclusively expressed in the human liver. OAT7 showed 35% to 46% identities to those of other members of the OAT family (50). When expressed in *Xenopus* oocytes, OAT7 mediated high-affinity transport of sulfate-conjugated steroid hormones, estrone sulfate (K_m = 8.7 μM) and DHEA sulfate (K_m = 2.2 μM), in a sodium-independent manner, whereas it did not transport other organic anions. Estrone sulfate transport mediated by OAT7 was inhibited by negatively charged BSP, ICG, and several sulfate-conjugated xenobiotics. In contrast, glucuronide and glutathione conjugates

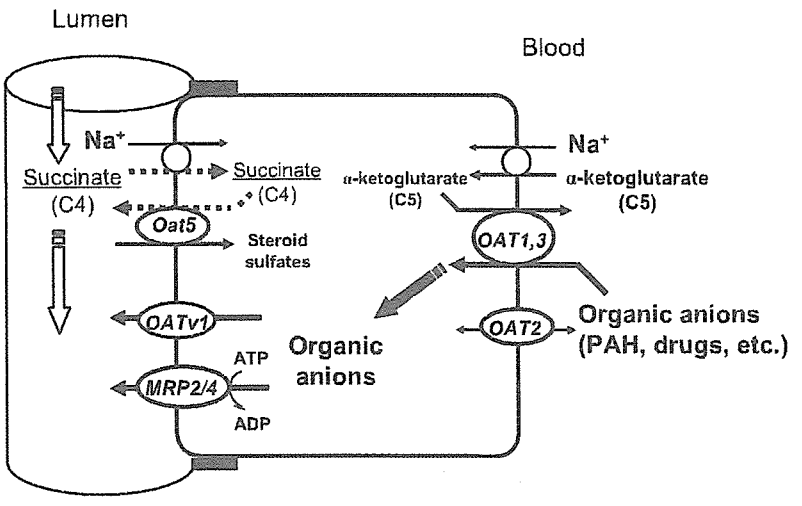

Fig. 2. Proposed scheme of organic anion transport coupling with two dicarboxylates in the proximal tubular cells.

exhibited no inhibitory effects on OAT7-mediated transport. Immunohistochemical analysis revealed that OAT7 protein was located in the sinusoidal membrane of hepatocytes.

Oat8: We identified a cDNA encoding a novel multispecific organic anion transporter (designated Oat8) from a rat kidney cDNA library (51). Oat8 showed 37% to 47% identities to other OAT family members. Oat8 mRNA is expressed exclusively in the kidney. When expressed in *Xenopus* oocytes, Oat8 mediated transport of sulfate conjugates of steroids such as estrone sulfate and DHEAS in a sodium-independent manner. Oat8 interacted with chemically heterogenous anionic compounds but not with the organic cation TEA. Oat8-mediated ES transport was inhibited by several sulfate conjugates, whereas glucuronide conjugates showed no inhibitory effects. Oat8 protein is localized in the collecting ducts.

OAT9: In a mouse EST database search, we found one EST clone that showed significant identity to OATs (52). This gene product shows approx. 36% identities to other OATs. Expression of OAT9 mRNA has been detected only in the kidney and brain. For functional analysis, we used proximal tubule cells (S2 cells) stably expressing OAT9. OAT9 mediated transport of nicotinic acid, salicylic acid, and PGE_2.

OAT-PG: In the kidney, prostaglandins (PGs), especially PGE_2, have important roles in renal hemodynamics, renin release, and tubular sodium and water reabsorption. Since PGs are charged organic anions at physiological pH, it is difficult for them to penetrate biological membranes. Accordingly, PG transport is a carrier-mediated process. So far, only prostaglandin transporter (PGT) from the OATP (SLCO/SLC21) family has been shown to be a transporter specific to PGs. We isolated a cDNA encoding a novel prostaglandin-specific transporter from the mouse kidney (53). Since this transporter belongs to the OAT family (SLC22) and is structurally distinct from PGT, we named it prostaglandin-specific organic anion transporter (OAT-PG). OAT-PG specifically mediated transport of PGs such as PGE_2 and $PGF_{2\alpha}$. OAT-PG mRNA is expressed exclusively in the kidney. We speculate that OAT-PG plays an important role in renal handling of PGE_2 and contributes to physiological functions involved in PGE_2 metabolism and signaling in the distal segments of nephrons.

3.3. Regulations

3.3.1. Phosphorylation

Organic anion transport in intact renal proximal tubular cells in animal model systems is downregulated by protein kinase C (PKC). All OAT isoforms cloned have several sites for PKC phosphorylation in the large intracellular loop between the sixth and seventh transmembrane domains. Several studies have revealed that the activation of PKC decreases the transport activity of OATs (54 – 59). This inhibitory effect is also associated with altered substrate selectivity. The reduced OAT-mediated transport activity is rescued by PKC inhibitors (54, 55). Furthermore, PKC-induced hOAT1 down-regulation is achieved via carrier retrieval from the cell membrane (58). In addition to the sites for phosphorylation by PKC, OAT isoforms have putative sites for phosphorylation by protein kinase A (PKA), casein kinase II, or tyrosine kinase. Among these, protein kinases, including mitogen-activated protein kinase (MAPK), PKA, and tyrosine kinase, have been shown to be involved in the regulation of OAT transport functions (59 – 61). Epidermal growth factor (EGF) stimulates PAH and estrone sulfate transport in rabbit renal proximal tubules via MAPKs, and PGE_2 enhances basolateral PAH and estrone sulfate uptake via adenylate cyclase activation and causes PKA activation (59, 60). A recent study has demonstrated that OAT3-mediated activity is also inhibited by tyrosine kinase and phosphatidylinositol 3-kinase (PI3K) (61).

3.3.2. Glycosylation

Glycosylation sites in the first extracellular loop between transmembrane domains (TMDs) 1 and 2 are conserved in OATs. Tunicamycin, an inhibitor of asparagine-linked glycosylation, inhibited PAH transport activity in mOat1-transfected COS7 cells (62). Immunofluorescence revealed that the mOat1 protein remained mainly in the intracellular compartment after tunicamycin treatment (62). That study indicates that glycosylation of the mOat1 protein is necessary for proper trafficking of the protein to the plasma membrane. Other experiments have demonstrated that disruption of Asp39 (one of the glycosylated sites) in mice resulted in complete loss of transport activity of OAT1 without affecting its surface expression (63). Thus, glycosylation could also be responsible for substrate recognition.

Recently, Zhou et al. investigated how the addition/acquisition and processing/modification of N-linked oligosaccharides play a role in the functional maturation of OAT4 using a novel approach (64). Inhibition of acquisition of oligosaccharides in OAT4 by mutating Asn to Gln and by tunicamycin treatment was combined with wild-type OAT4 expression in a series of mutant CHO-Lec cells defective in different steps of glycosylation processing. Zhou et al. demonstrated that both the disruption of glycosylation sites by mutagenesis and the inhibition of glycosylation by tunicamycin treatment

resulted in a nonglycosylated OAT4, which was unable to target to the cell surface. In contrast, OAT4 synthesized in mutant CHO-Lec cells carrying different structural forms of sugar moieties (mannose-rich in Lec1 cells, sialic acid-deficient in Lec2 cells, and sialic acid/galactose-deficient in Lec8 cells) was able to traffic to the cell surface. However, OAT4 expressed in CHO-Lec1 cells had significantly lower binding affinity for its substrates than did that expressed in parental CHO cells. These results provided novel information that addition/acquisition of oligosaccharides but not the processing of added oligosaccharides participates in the membrane insertion of OAT4. Processing of added oligosaccharides from mannose-rich type to complex type is important for enhancing the binding affinity of OAT4 for its substrates. Glycosylation could therefore serve as a means to specifically regulate OAT4 function in vivo.

3.3.3. Transcriptional regulation

Eraly et al. (65) investigated regulatory elements using comparative genomics approaches. Binding sites for transcription factors, including PAX1, PBX, WT1, and HNF1, are present within the evolutionarily conserved noncoding sequences of OATs, although the roles of these transcription factors in expression of OATs have not been clarified.

The cloning and preliminary characterization of a human urate transporter (hURAT1) gene promoter was reported by Li et al. (66). The transcription initiation site was mapped to a base 337-bp upstream of the ATG start codon by primer extension and 5'-RACE. The minimal functional promoter region was within 253 bp when promoter/luciferase constructs were transfected into OK cells. Testosterone significantly increased promoter activity, suggesting that hormonal regulation of hURAT1 is the cause of gender differences in blood urate levels.

Recently, *cis*-acting elements in the 5'-flanking region that regulate hOAT2 transcription were characterized by Popowski et al. (67). A consensus binding motif for the hepatocyte nuclear factor-4α (HNF-4α) is located at nucleotides $-329/-317$ relative to the transcription initiation site. A luciferase-linked hOAT2 promoter fragment containing the HNF-4α binding site was transactivated with co-expression of HNF-4α in Huh7 cells, whereas site-directed mutagenesis of the DR-1 element abolished activation by HNF-4α. SiRNAs inhibiting endogenous HNF-4α expression markedly reduced endogenous hOAT2 expression in Huh7 cells. Since HNF-4α is a known target for bile acid-mediated repression of gene transcription, Popowski et al. investigated whether chenodeoxycholic acid (CDCA) suppresses hOAT2 gene expression by inhibiting HNF-4α-mediated transactivation. Treatment of Huh7 cells with CDCA or the synthetic farnesoid X receptor (FXR) agonist GW4064 decreased mRNA and protein levels and also nuclear binding activity of HNF-4α. The FXR-inducible transcriptional repressor small heterodimer partner inhibited transactivation of hOAT2 promoter constructs and of endogenous hOAT2 expression by HNF-4α. They concluded that the hOAT2 gene is critically dependent on HNF-4α and that bile acids repress the hOAT2 gene by inhibiting HNF-4α. Hepatic uptake of hOAT2 substrates may thus be decreased in disease conditions associated with elevated intracellular levels of bile acids.

3.3.4. Gender differences

Gender differences in mRNA and/or protein expression have been reported for Oat1 (68, 69), Oat2 (69–71), Oat3 (68, 69, 71), and Urat1 (72), suggesting that some OAT family members are regulated by sex hormones. The mouse Oat1 mRNA levels were found to be higher in the male kidney than in the female kidney, and the rat Oat2 mRNA expression level was found to be higher in the female kidney than in the male kidney or liver. In contrast, the mouse Oat2 mRNA levels were found to be high in both male and female kidneys and low in the male liver. Rat Oat3 mRNA expression was detected in the male liver. The mouse Urat1 mRNA levels were found to be higher in the male kidney than in the female kidney.

3.3.5. Ontogenic expression

Developmental changes in expression of OATs have been reported (69, 73, 74): the mRNA expression levels of Oat1, Oat2, and Oat3 increased during postnatal development.

3.3.6. Pathophysiological status

Recent studies have indicated that the expressions of OATs are affected in pathophysiological states. During the progression of renal insufficiency, various uremic toxins derived from dietary proteins accumulate in uremic plasma. Many uremic toxins are organic anions; their accumulation in the kidney is a result of renal dysfunction, and this also accelerates underlying renal diseases. Enomoto et al. (75) demonstrated that the administration of indoxyl sulfate (IS) into nephrectomized rats enhanced the progression of chronic renal failure. Immunohistochemical studies revealed that the amount of IS in proximal tubular cells and the expression of OAT1 and OAT3 are both increased in a chronic renal failure model. Deguchi et al. (76) analyzed the transport of various uremic toxins, such as IS, 3-carboxy-

4-methyl-5-propyl-2-furanpropionate, indole acetate, and hippurate, via OAT1 and OAT3. They showed that rOat1/hOAT1 and rOat3/hOAT3 play major roles in the renal uptake of these uremic toxins. The enhanced expression of OATs in uremic circumstances indicates compensatory effects for elimination of uremic substrances and leads to progress of the underlying diseases by accumulation of harmful uremic toxins in proximal tubular cells. The expressions of OATs are affected by several renal dysfunction models. Bilateral urethral obstruction in adult male rats decreases Oat1 and Oat3 expression levels in basolateral membrane fractions in the kidney (77). Acute arterial calcinosis induced by bolus injection of vitamin D3 also increases the Oat1 expression level (78). OAT expression in various human kidney diseases, was analyzed using a real-time PCR method (79). The data indicate that OAT3 expression is decreased in patients with renal diseases. OAT expression is influenced not only by renal diseases but also by hepatic diseases. A compensatory enhancement of organic anion excretion in rats with acute biliary obstruction was demonstrated for OAT1 and OAT3 (80). In a rat model of fever generation in which peripheral PGE_2 is increased and clearance by metabolism of peripheral PGE_2 is downregulated, PGE_2 not only time-dependently downregulates basolateral organic anion uptake but also diminishes expression of both rOat1 and rOat3 (81). These results suggest that during fever or inflammation, renal secretory transport of PGE_2 is reduced, contributing to elevated PGE_2 levels in blood. The significance and relevance of changes in OAT expression in pathophysiological states are an important issue for future studies.

3.4. Structure-function relations

Site-directed mutagenesis studies revealed that the following residues are important for substrate recognition: His34, Lys394, and Arg478 in flounder Oat1 (82) and Lys370 and Arg454 in rOat3 (83). Recently, information regarding functionally critical amino acid residues has been increasing.

OAT1: An alanine scanning mutagenesis study revealed that residues Leu-30 and Thr-36 are important for OAT1 transport activities (84). Progressively smaller side chains at position 30 increasingly impaired hOAT1 function mainly because of the impaired surface expression of the transporter. Substitution of Thr-36 by serine and cysteine at this position abolished transport activity without affecting the surface expression of the transporter. These results indicate that both the methyl group and the hydroxyl group of Thr-36 could be critical for hOAT1 activity.

The cysteine-modifying reagent *p*-chloromercuribenzenesulphonate (PCMBS) inhibits mOat1-mediated PAH transport in HeLa cells (85). Site-directed mutagenesis studies revealed that single replacement of cysteine residues had no significant effect on mOat1-mediated PAH transport but that multiple replacements in the C-terminal region (C335/379/427/434A; Cys335/379/427/434Ala) resulted in a substantial decrease in transport activity. A simultaneous replacement of all 13 cysteine residues (C-less) led to a complete loss of transport function. The decrease in or lack of transport activity of the mutants C335/379/427/434A and C-less was due to the impaired trafficking of the mutant transporters to the cell surface. These results suggest that although cysteine residues are not required for function in mOat1, their presence appears to be important for targeting of the transporter to the plasma membrane. Since C49A was less sensitive than the wild-type mOat1, the modification of Cys49 may play a role in the inhibition of mOat1 by PCMBS.

Hong et al. first demonstrated that hOAT1 exists in the plasma membrane as a homooligomer (86). They investigated the quaternary structure of hOAT1 using combined approaches of chemical cross-linking, gel filtration chromatography, co-immunoprecipitation, cell surface biotinylation, and metabolic labeling.

OAT4: The histidine-modifying reagent diethyl pyrocarbonate (DEPC) inhibitied OAT4-mediated estrone sulfate transport in COS-7 cells (87). Single replacement of His (H)-47 or simultaneous replacement of H47/52/83 or H47/52/83/305/469 to Ala by site-directed mutagenesis led to a 50%–80% decrease in transport activity. The decreased transport activity of these mutants was correlated with a decreased amount of cell surface expression. These results suggest that mutation at positions 47, 47/52/83 and 47/52/83/305/469 impaired membrane expression rather than function. Since H469A mutant lacks sensitivity to DEPC inhibition, the modification of His-469 seems to be responsible for the inhibition of OAT4 by DEPC.

The role of conserved glycine residues in OAT4 function was investigated by Zhou et al. (88). Mutants G11S, G383S, G388S, and G466S exhibited transport activities comparable with those of wild-type OAT4, while mutants G241S and G400S had almost completely lost transport function. They then demonstrated that increasingly larger side chains at positions 241 and 400 increasingly impaired OAT4 function. Cell-surface biotinylation showed that mutations of Gly-241 and Gly-400 interfered with the trafficking of the transporter to the cell surface. Substitutions of amino acids with large side chains at positions 241 and 400 resulted in decreased V_{max} and increased K_m. These results suggest that Gly-241 and Gly-400 are important both in targeting

the transporter to the plasma membrane and in substrate binding.

3.5. Targeted disruption

The generation of gene knockout animals could provide new information on the contribution of individual transporters in intact organs. Knockout mice for Oat1 (89) and Oat3 (26) have been generated. Both models revealed the loss of organic anion transport and indicated the importance of drug uptake of Oat1 in the kidney (89) and of Oat3 in kidney (26) and choroids plexus (90), although they showed no morphological changes.

3.6. Drug-drug interactions

Drugs present in plasma could affect the transport of the drugs individually and could mutually influence the pharmacokinetics of the drugs. A notable example is the concomitant use of probenecid and penicillin G; the half-life of penicillin G is significantly prolonged when combined with probenecid compared with when it is administered alone. It has also been reported that the administration of methotrexate (MTX) with acidic drugs, such as NSAIDs, and β-lactam antibiotics causes severe suppression of bone marrow. NSAIDs and β-lactam antibiotics inhibit the tubular secretion of MTX, thereby reducing its renal clearance. As a consequence, unwanted side-effects, such as bone marrow suppression, could occur as a result of the increase in plasma MTX levels (91, 92). An extensive review on OAT-mediated drug-drug interactions is available (93).

3.7. Polymorphisms

In addition to drug-metabolizing enzymes, drug transporters play important roles in determining the pharmacokinetic profiles of drugs and their pharmacological effects. Recent wide-scale sequencing analysis of the human genome has lead to identification of the single nucleotide polymorphisms (SNPs) of drug transporters. It has been suggested that drug transporter SNPs are responsible for the interindividual variation in drug elimination from the body (94). Recently, two groups reported results of functional analysis of non-synonymous variants of hOAT1 genes (95, 96). Fujita et al. found six non-synonymous variants of hOAT1 (95). Two variants (R50H and R293W) exhibited normal uptake of PAH, ochratoxin A, and methotrexate assayed in *Xenopus* oocytes. One variant, R454Q, was non-functional with respect to the above substrates. In a clinical study, no significant decrease was found between renal secretory clearance of adefovir in family members heterozygous for hOAT1-454Q and in those with the reference transporter, hOAT1-454R. Bleasby et al. found twenty hOAT1 SNPs from genomic DNA from 92 individuals of African, Asian, and Caucasian origin (96). Among them, two SNPs encoded changes in the amino acid sequence: R50H and K293I. These SNPs were only present in samples of African origin. When expressed in *Xenopus* oocytes, wild-type R50-hOAT1 and the variants R50H-hOAT1 and K525I-hOAT1 all mediated probenecid-sensitive PAH uptake. Kinetic analysis indicated that the transport affinity (K_m) for PAH was unchanged in the variants compared with that in the wild type. Interestingly, the Km for the nucleoside phosphonate analogs adefovir, cidofovir, and tenofovir seemed to be decreased in the R50H variant compared with that in the wild type, whereas the kinetics of K525I remained unchanged. Studies on human drug transporter SNPs have been started, and accumulation of such information should lead to the establishment of individualized drug therapy in the future.

3.8. Protein-protein interaction

It has been demonstrated that several transporters located in the apical membrane of proximal tubular cells possess a PDZ motif at their COOH-terminal end (6, 97). The PDZ motif is one of the protein-protein interaction modules and is composed of three amino acid residues: S/T-X-Φ (where X is any amino acid and Φ is a hydrophobic residue). The renal apical organic anion transporters OAT4 and URAT1 possess the PDZ motif at their C-terminus. Yeast two-hybrid experiments revealed that both OAT4 and URAT1 interact with the multivalent PDZ domain-containing protein PDZK1 via their C-terminal PDZ motifs (98, 99). The coexpression of URAT1/OAT4 and PDZK1 in HEK293 cells increases URAT1/OAT4 transport activity. This synergic effect is abolished when the C-terminal PDZ motif deletion mutant of URAT1/OAT4 is coexpressed with PDZK1. These results indicate that PDZK1 regulates transport activities via interaction with the PDZ motif.

To date, four PDZ proteins, Na^-/H^- exchanger regulatory factor (NHERF)1, NHERF2, PDZK1 (NHERF3), and intestinal and kidney-enriched PDZ protein IKEPP (NHERF4), have been identified in the apical membrane of renal proximal tubular cells (97). We also found that OAT4 interacts with NHERF1 and that the coexpression of OAT4 and PDZK1 in HEK293 cells increases OAT4-mediated estrone sulfate transport activity (99). NHERF1 and PDZK1 have been shown to interact with several organic anion transporters such as Na^--dependent phosphate cotransporter type 1 (NPT1), MRP2, and MRP4. Since PDZK1 and NHERF1 can bind to each other, both PDZK1 and NHERF1 may organize the scaffold network and tether several apical transporters simultaneously in the apical membrane of

renal proximal tubular cells.

In kidneys, the proximal tubule has important roles in both the reabsorption of filtered substances and the secretion of water-soluble drugs, toxins, and metabolic waste products. These two opposite transport directions are simultaneously accomplished by the coordinated action of ion channels and transporters located both in the apical membrane and basolateral membrane. Thus, the polarized expression of these membrane proteins is essential for the function of proximal tubular cells. Scaffolding proteins underneath the plasma membrane, such as PDZ proteins, are thought to contribute to the generation of cell polarity by the formation of a junctional complex and by protein anchoring. In addition, proximal tubular transport processes are regulated by a number of factors, including hormones such as parathyroid hormone. For efficient and specific signal transduction, for the enhancement of membrane expression, and for the direct modulation of transport processes, the formation of functional complexes, including transport proteins, hormonal receptors, and intracellular signaling elements, is beneficial. This supramolecular structure, namely "Transportsome", supported by scaffolds such as PDZ proteins, is proposed to be an ultimate functional unit of membrane transport.

Besides PDZ proteins, a novel protein that modulates transporter activities has been identified. A new ischemia/reperfusion-inducible protein (IRIP), which belongs to the SUA5/YrdC/YciO protein family, was isolated in a differential display analysis of an ischemia /reperfusion-treated kidney RNA sample (100). Mouse IRIP mRNA was expressed in all tissues tested, the highest levels being in the testis and in secretory and endocrine organs. Besides ischemia/reperfusion, endotoxemia also activated the expression of IRIP in the liver, lung, and spleen. The transporter regulator RS1, which was originally isolated from an expression cDNA library of porcine kidney cortex by screening the library with a monoclonal antibody that stimulated high-affinity phloridzin binding, was identified as an IRIP-interacting protein in yeast two-hybrid assays and coimmunoprecipitation assays. IRIP overexpression inhibited endogenous 1-methyl-4-phenylpyridinium (MPP^+) uptake activity in HeLa cells. The activities of exogenous organic cation transporters (OCT2 and OCT3), organic anion transporter (OAT1), and monoamine transporters were also inhibited by IRIP. IRIP is thought to regulate the activities of a variety of transporters under normal and pathological conditions.

3.9. Protein-lipid interaction

Localization is a major issue for membrane proteins, since their recruitment to the plasma membrane is a prerequisite for various functions of the proteins. Within the plasma membrane, correct localization is equally important, since a recent study has shown that the membrane itself is highly organized into lipid domains that provide subcompartments. These small (<100 nm) membrane domains, also called rafts, are enriched in sphingolipids and cholesterol and incorporate GPI-anchored proteins, specific transmembrane proteins, and doubly acylated proteins such as tyrosine kinases of the Src family. Rafts have been proposed to function as platforms for the assembly of cytoplasmic and membranous signaling molecules and for polarized membrane traffic. Caveolae represent a subpopulation of lipid rafts that contain the scaffolding protein caveolin, which can organize the assembly of macromolecular complexes and regulate protein function within caveolae (101). Three caveolin genes (Cav-1, Cav-2, and Cav-3) have been identified. Cav-1 and Cav-2 have a wide distribution among different cell types, whereas Cav-3 is expressed exclusively in all types of muscle. Since caveolin (Cav) is known to play a role in membrane transport, interactions between transporters and caveolins are an important issue. Kwak et al. demonstrated that rOat1 and Cav-2 are co-expressed in the plasma membrane and that rOat1's function for organic anion transport is upregulated by Cav-2 in physiological conditions (102). Kwak et al. also showed that rOat3 and Cav-1 share cellular expression in the plasma membrane and that Cav-1 upregulates the organic anion uptake via rOat3 under physiological conditions (103).

3.10. Novel aspects of OATs

Recently, receptors for dicarboxylates such as succinate and α-ketoglutarate have been identified in the kidneys (104). Succinate is a natural ligand for GPR91, and α-ketoglutarate is a natural ligand for GPR99, orphan G-protein-coupled receptors (GPCRs) in proximal and distal tubules. He et al. showed that succinate increases blood pressure in mice and that the succinate-induced hypertension involves the renin-angiotensin system. These findings suggest that the level of dicarboxylates surrounding proximal tubular cells, determined by the balance between the uptake of dicarboxylates via Na^+-dependent dicarboxylate transporters (NaDCs) (105) and their efflux via OATs, is an important factor that regulates renovascular hypertension. In the earlier part of this review, we proposed by taking into account the existence of the outwardly directed dicarboxylate gradient in tubular cells that OAT4 contributes to the tubular reabsorption of organic anions. However, not only the organic anion influx but also the dicarboxylate efflux seems to have important

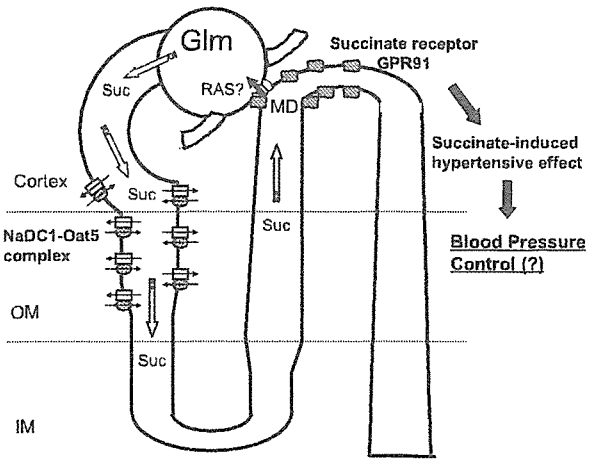

Fig. 3. Succinate as a signaling molecule in the kidney. Suc: succinate, Glm: glomerulus, OM: outer medulla, IM: inner medulla, MD: macula densa, RAS: rennin-aldosterone system.

roles for OAT family members, because no other transport protein mediating dicarboxylate efflux has been identified to date. Due to the function of apical organic anion-transporting multimolecular complex (organic anion transportsome), dicarboxylates remaining in the tubular fluid go down to the distal nephron and function as a signaling molecule for renovascular hypertension, a disease closely linked to atherosclerosis, diabetes, and renal failure. Therefore, apical organic anion transportsome can function as a regulator of dicarboxylate signaling and it could be a novel therapeutic target for the above-stated diseases (Fig. 3).

The role of the efflux pathway for OATs seems also to be important in endocrine tissues. It has been suggested that OAT1 is involved in cortisol release from bovine and rat adrenal zona fasciculata cells, but there is no information on the existence of OATs in human adrenal cells. Asif et al. addressed the question of whether OATs are present in human adrenal cortical cells using the human adrenal cell line NCI-H295R established in 1990 from a patient with adrenocortical carcinoma who showed high rate of secretion of mineralcorticoids, glucocorticoids, and androgen (106). RT-PCR did not reveal expression of hOAT1 and hOAT2, but hOAT3 and hOAT4 mRNAs were detected in both NCI-H295R cells and human adrenal tissue. When human OAT3 (hOAT3) and hOAT4 were expressed in *Xenopus* oocytes, only hOAT3 showed [^{3}H]cortisol uptake in excess of that of water-injected control oocytes. In NCI-H295R cells, [^{3}H]estrone sulfate uptake was saturable, *cis*-inhibited by OAT substrates, and *trans*-stimulated by preloading with glutarate or cortisol. Likewise, [^{3}H]PAH uptake was *cis*-inhibited by estrone sulfate and *trans*-stimulated by preloading the cells with PAH, glutarate, or cortisol, indicating functional expression of OATs in the plasma membrane of NCI-H295R cells. Therefore, in addition to the well known role of OATs in the elimination of organic anions from the body, the maintenance and regulation of endocrine functions would be another important role of them.

4. Perspectives

In this review, we describe recent progress in the understanding of various aspects of the OAT family (SLC22). Characterization of the OAT family members has brought us a step further in the elucidation of molecular mechanisms for drug elimination and distribution in the kidneys, liver, and brain. Nonetheless, many questions remain to be answered. First, several uncharacterized (orphan) transporters in the SLC22A superfamily remain, and further investigation is therefore required to determine their functions. Second, knowledge of the mechanisms by which OATs are regulated is lacking. Gender differences in the expression levels of OAT family members are of significant interest. Third, clarification of the three-dimensional (3D) structures of OATs is necessary to understand the broad substrate recognition of OATs. Because of difficulties in the purification and crystallization of membrane transporter proteins, the 3D structures of transporters have yet to be clarified. Fourth, a comprehensive understanding of the apical exit pathway for organic anions in the kidneys and the PDZ interaction on apical OATs is an important issue. Finally, the pathological significance of OATs is of great interest. Originally, studies on OATs were focused on the molecular mechanisms that underlie the elimination of xenobiotics. However, recent studies have unveiled the reabsorptive roles of endogenous compounds, such as urate, for OAT isoforms. This implies that the fundamental roles of OATs are not restricted to pharmacological and toxicological roles. Thus, genetic defects of OATs might give rise to pathophysiological states.

Acknowledgments

The authors wish to thank all of the members of their laboratories who have contributed to much of the work discussed in this review. This work was supported in part by grants from the Ministry of Education, Culture, Sports, Science, and Technology of Japan; the Japan Society for the Promotion of Science, Research on Health Sciences focusing on Drug Innovation from the Japan Health Sciences Foundation; Mutual Aid Corpora-

tion for Private Schools of Japan; the Salt Science Research Foundation (No. 0524); the Japan Foundation of Applied Enzymology; Astellas Foundation for Research on Metabolic Disorders; Gout Research Foundation of Japan; Kyorin University School of Medicine (Kyorin Medical Research Award 2006); and Health and Labor Sciences Research Grants for Research on Advanced Medical Technology: Toxicogenomics Project.

References

1 Marshall EK Jr, Vickers JL. The mechanism of the elimination of phenolsulphonephthalein by the kidney – a proof of secretion by the convoluted tubules. Johns Hopkins Hosp (Bull). 1923; 34:1–6.
2 Ullrich KJ. Renal transporters for organic anions and organic cations. Structural requirements for substrates. J Memb Biol. 1997;158:95–107.
3 Pritchard JB, Miller DS. Mechanisms mediating renal secretion of organic anions and cations. Physiol Rev. 1993;73:765–796.
4 Moller JV, Sheikh MI. Renal organic anion transport system: pharmacological, physiological, and biochemical aspects. Pharmacol Rev. 1982;34:315–358.
5 Inui KI, Masuda S, Saito H. Cellular and molecular aspects of drug transport in the kidney. Kidney Int. 2000;58:944–958.
6 Russel FG, Masereeuw R, van Aubel RA. Molecular aspects of renal anionic drug transport. Annu Rev Physiol. 2002;64:563–594.
7 Miyazaki H, Sekine T, Endou H. The multispecific organic anion transporter family: properties and pharmacological significance. Trends Pharmacol Sci. 2004;25:654–662.
8 Burckhardt BC, Burckhardt G. Transport of organic anions across the basolateral membrane of proximal tubule cells. Rev Physiol Biochem Pharmacol. 2003;146:95–158.
9 Wright SH, Dantzler WH. Molecular and cellular physiology of renal organic cation and anion transport. Physiol Rev. 2004;84: 987–1049.
10 Sekine T, Watanabe N, Hosoyamada M, Kanai Y, Endou H. Expression cloning and characterization of a novel multispecific organic anion transporter. J Biol Chem. 1997;272:18526–18529.
11 Sweet DH, Wolff NA, Pritchard JB. Expression cloning and characterization of ROAT1. The basolateral organic anion transporter in rat kidney. J Biol Chem. 1997;272:30088–30095.
12 Wolff NA, Werner A, Burkhardt S, Burckhardt G. Expression cloning and characterization of a renal organic anion transporter from winter flounder. FEBS Lett. 1997;417:287–291.
13 Shimada H, Moewes B, Burckhardt G. Indirect coupling to Na^+ of p-aminohippuric acid uptake into rat renal basolateral membrane vesicles. Am J Physiol. 1987;253:F795–F801.
14 Kusuhara H, Sekine T, Utsunomiya-Tate N, Tsuda M, Kojima R, Cha SH, et al. Molecular cloning and characterization of a new multispecific organic anion transporter from rat brain. J Biol Chem. 1999;274:13675–13680.
15 Sekine T, Cha SH, Endou H. The multispecific organic anion transporter (OAT) family. Pflugers Arch. 2000;440:337–350.
16 Habu Y, Yano I, Hashimoto Y, Saito H, Inui K. p-Aminohippurate transport at the apical membrane in the OK kidney epithelial cell line. Pharm Res. 2002;19:1822–1826.
17 Dantzler WH. Renal organic anion transport: a comparative and cellular perspective. Biochim Biophys Acta 2002;1566:169–181.
18 Simonson GD, Vincent AC, Roberg KJ, Huang Y, Iwanij V. Molecular cloning and characterization of a novel liver-specific transport protein. J Cell Sci. 1994;107:1065–1072.
19 Sekine T, Cha SH, Tsuda M, Apiwattanakul N, Nakajima N, Kanai Y, et al. Identification of multispecific organic anion transporter 2 expressed predominantly in the liver. FEBS Lett. 1998;429:179–182.
20 Babu E, Takeda M, Narikawa S, Kobayashi Y, Yamamoto T, Cha SH, et al. Human organic anion transporters mediate the transport of tetracycline. Jpn J Pharmacol. 2002;88:69–76.
21 Kobayashi Y, Ohshiro N, Sakai R, Ohbayashi M, Kohyama N, Yamamoto T. Transport mechanism and substrate specificity of human organic anion transporter 2 (hOat2 [SLC22A7]). J Pharm Pharmacol. 2005;57:573–578.
22 Brady KP, Dushkin H, Fornzler D, Koike T, Magner F, Her H, et al. A novel putative transporter maps to the osteosclerosis (oc) mutation and is not expressed in the oc mutant mouse. Genomics. 1999;56:254–261.
23 Cha SH, Sekine T, Fukushima JI, Kanai Y, Kobayashi Y, Goya T, et al. Identification and characterization of human organic anion transporter 3 expressing predominantly in the kidney. Mol Pharmacol. 2001;59:1277–1286.
24 Kojima R, Sekine T, Kawachi M, Cha SH, Suzuki Y, Endou H. Immunolocalization of multispecific organic anion transporters, OAT1, OAT2, and OAT3, in rat kidney. J Am Soc Nephrol. 2002;13:848–857.
25 Nagata Y, Kusuhara H, Endou H, Sugiyama Y. Expression and functional characterization of rat organic anion transporter 3 (rOat3) in the choroid plexus. Mol Pharmacol. 2002;61:982–988.
26 Sweet DH, Miller DS, Pritchard JB, Fujiwara Y, Beier DR, Nigam SK. Impaired organic anion transport in kidney and choroid plexus of organic anion transporter 3 (Oat3 (Slc22a8)) knockout mice. J Biol Chem. 2002;277:26934–26943.
27 Ohtsuki S, Kikkawa T, Mori S, Hori S, Takanaga H, Otagiri M, et al. Mouse reduced in osteosclerosis transporter functions as an organic anion transporter 3 and is localized at abluminal membrane of blood-brain barrier. J Pharmacol Exp Ther. 2004;309:1273–1281.
28 Sweet DH, Chan LM, Walden R, Yang XP, Miller DS, Pritchard JB. Organic anion transporter 3 (Slc22a8) is a dicarboxylate exchanger indirectly coupled to the Na+ gradient. Am J Physiol Renal Physiol. 2003;284:F763–F769.
29 Bakhiya A, Bahn A, Burckhardt G, Wolff N. Human organic anion transporter 3 (hOAT3) can operate as an exchanger and mediate secretory urate flux. Cell Physiol Biochem. 2003;13: 249–256.
30 Cha SH, Sekine T, Kusuhara H, Yu E, Kim JY, Kim DK, et al. Molecular cloning and characterization of multispecific organic anion transporter 4 expressed in the placenta. J Biol Chem. 2000;275:4507–4512.
31 Ugele B, St-Pierre MV, Pihusch M, Bahn A, Hantschmann P. Characterization and identification of steroid sulfate transporters of human placenta. Am J Physiol Endocrinol Metab. 2003;284: E390–E398.
32 Ekaratanawong S, Anzai N, Jutabha P, Miyazaki H, Noshiro R,

Takeda M, et al. Human organic anion transporter 4 is a renal apical organic anion/dicarboxylate exchanger in the proximal tubules. J Pharmacol Sci. 2004;94:297–304.

33 Enomoto A, Kimura H, Chairoungdua A, Shigeta Y, Jutabha P, Cha SH, et al. Molecular identification of a renal urate anion exchanger that regulates blood urate levels. Nature. 2002;417: 447–452.

34 Alebouyeh M, Takeda M, Onozato ML, Tojo A, Noshiro R, Hasannejad H, et al. Expression of human organic anion transporters in the choroid plexus and their interactions with neurotransmitter metabolites. J Pharmacol Sci. 2003;93:430–436.

35 Mori S, Takanaga H, Ohtsuki S, Deguchi T, Kang YS, Hosoya K, et al. Rat organic anion transporter 3 (rOAT3) is responsible for brain-to-blood efflux of homovanillic acid at the abluminal membrane of brain capillary endothelial cells. J Cereb Blood Flow Metab. 2003;23:432–440.

36 Ohtsuki S, Kikkawa T, Mori S, Hori S, Takanaga H, Otagiri M, et al. Mouse reduced in osteosclerosis transporter functions as an organic anion transporter 3 and is localized at abluminal membrane of blood-brain barrier. J Pharmacol Exp Ther. 2004;309:1273–1281.

37 Bahn A, Ljubojevic M, Lorenz H, Schultz C, Ghebremedhin E, Ugele B, et al. Murine renal organic anion transporters mOAT1 and mOAT3 facilitate the transport of neuroactive tryptophan metabolites. Am J Physiol Cell Physiol. 2005;289:C1075–C1084.

38 Mori S, Ohtsuki S, Takanaga H, Kikkawa T, Kang YS, Terasaki T. Organic anion transporter 3 is involved in the brain-to-blood efflux transport of thiopurine nucleobase analogs. J Neurochem. 2004;90:931–941.

39 Kobayashi Y, Ohshiro N, Tsuchiya A, Kohyama N, Ohbayashi M, Yamamoto T. Renal transport of organic compounds mediated by mouse organic anion transporter 3 (mOat3): further substrate specificity of mOat3. Drug Metab Dispos. 2004;32: 479–483.

40 Hashimoto T, Narikawa S, Huang XL, Minematsu T, Usui T, Kamimura H, et al. Characterization of the renal tubular transport of zonampanel, a novel alpha-amino-3-hydroxy-5-methylisoxazole-4-propionic acid receptor antagonist, by human organic anion transporters. Drug Metab Dispos. 2004;32:1096–1102.

41 Rengelshausen J, Lindenmaier H, Cihlar T, Walter-Sack I, Haefeli WE, Weiss J. Inhibition of the human organic anion transporter 1 by the caffeine metabolite 1-methylxanthine. Biochem Biophys Res Commun. 2004;320:90–94.

42 Sugawara M, Mochizuki T, Takekuma Y, Miyazaki K. Structure-affinity relationship in the interactions of human organic anion transporter 1 with caffeine, theophylline, theobromine and their metabolites. Biochim Biophys Acta. 2005;1714:85–92.

43 Hasegawa M, Kusuhara H, Sugiyama D, Ito K, Ueda S, Endou H, et al. Functional involvement of rat organic anion transporter 3 (rOat3; Slc22a8) in the renal uptake of organic anions. J Pharmacol Exp Ther. 2002;300:746–753.

44 Khamdang S, Takeda M, Shimoda M, Noshiro R, Narikawa S, Huang XL, et al. Interactions of human- and rat-organic anion transporters with pravastatin and cimetidine. J Pharmacol Sci. 2004;94:197–202.

45 He X, Anzai N, Ueno T, Fukutomi T, Sakata T, Endou H, et al. Trasport of nicotinate by human organic anion transporter hOAT2 and its possible interaction with transport of salicylate [abstract]. J Pharmacol Sci. 2006;100 Suppl I:126P.

46 Youngblood GL, Sweet DH. Identification and functional assessment of the novel murine organic anion transporter Oat5 (Slc22a19) expressed in kidney. Am J Physiol Renal Physiol. 2004;287:F236–F244.

47 Anzai N, Jutabha P, Enomoto A, Yokoyama H, Nonoguchi H, Hirata T, et al. Functional characterization of rat organic anion transporter 5 (Slc22a19) at the apical membrane of renal proximal tubules. J Pharmacol Exp Ther. 2005;315:534–544.

48 Sun W, Wu RR, van Poelje PD, Erion MD. Isolation of a family of organic anion transporters from human liver and kidney. Biochem Biophys Res Commun. 2001;283:417–422.

49 Monte JC, Nagle MA, Eraly SA, Nigam SK. Identification of a novel murine organic anion transporter family member, OAT6, expressed in olfactory mucosa. Biochem Biophys Res Commun. 2004;323:429–436.

50 Shin HJ, Anzai N, Enomoto A, Kim DK, Kanai Y, Endou H. Functional characterization and tissue localization of SLC22 organic anion transporter OAT7 [abstract]. J Pharmacol Sci. 2005;97 Suppl I:201P.

51 Yokoyama H, Anzai N, Chaekuntode S, Shin HJ, Noshiro R, Miyazaki H, et al. Identification of a novel organic anion transporter OAT8 from the rat kidney [abstract]. Nephrol Dial Transpl. 2003;18:S8.

52 Hirata T, Ellapan B, Anzai N, He X, Endou H, Kanai Y. Molecular identification and functional characterization of a novel organic anion trasporter OAT9 that is expressed in brain and kidney [abstract]. J Pharmacol Sci. 2006;100 Suppl I:98P.

53 Anzai N, Shiraya K, Hirata T, Jutabha P, Hatano R, Sanada S, et al. Identification and characterization of a novel renal prostaglandin-specific organic anion trasporter (OAT-PG) structurally distinct from PGT [abstract]. J Pharmacol Sci. 2006;100 Suppl I:111P.

54 Lu R, Chan BS, Schuster VL. Cloning of the human kidney PAH transporter: narrow substrate specificity and regulation by protein kinase C. Am J Physiol. 1999;276:F295–F303.

55 Uwai Y, Okuda M, Takami K, Hashimoto Y, Inui K. Functional characterization of the rat multispecific organic anion transporter OAT1 mediating basolateral uptake of anionic drugs in the kidney. FEBS Lett. 1998;438:321–324.

56 You G, Kuze K, Kohanski RA, Amsler K, Henderson S. Regulation of mOAT-mediated organic anion transport by okadaic acid and protein kinase C in LLC-PK$_1$ cells. J Biol Chem. 2000;275: 10278–10284.

57 Takeda M, Sekine T, Endou H. Regulation by protein kinase C of organic anion transport driven by rat organic anion transporter 3 (rOAT3). Life Sci. 2000;67:1087–1093.

58 Wolff NA, Thies K, Kuhnke N, Reid G, Friedrich B, Lang F, et al. Protein kinase C activation downregulates human organic anion transporter 1-mediated transport through carrier internalization. J Am Soc Nephrol. 2003;14:1959–1968.

59 Soodvilai S, Chatsudthipong V, Evans KK, Wright SH, Dantzler WH. Acute regulation of OAT3-mediated estrone sulfate transport in isolated rabbit renal proximal tubules. Am J Physiol Renal Physiol. 2004;287:F1021–F1029.

60 Sauvant C, Hesse D, Holzinger H, Evans KK, Dantzler WH, Gekle M. Action of EGF and PGE_2 on basolateral organic anion uptake in rabbit proximal renal tubules and hOAT1 expressed in human kidney epithelial cells. Am J Physiol Renal Physiol.

2004;286:F774–F783.
61 Soodvilai S, Wright SH, Dantzler WH, Chatsudthipong V. Involvement of tyrosine kinase and PI3K in the regulation of OAT3-mediated estrone sulfate transport in isolated rabbit renal proximal tubules. Am J Physiol Renal Physiol. 2005;289: F1057–F1064.
62 Kuze K, Kuze K, Graves P, Leahy A, Wilson P, Stuhlmann H, et al. Heterologous expression and functional characterization of a mouse renal organic anion transporter in mammalian cells. J Biol Chem. 1999;274:1519–1524.
63 Tanaka K, Tanaka K, Xu W, Zhou F, You G. Role of glycosylation in the organic anion transporter OAT1. J Biol Chem. 2004;279:14961–14966.
64 Zhou F, Xu W, Hong M, Pan Z, Sinko PJ, Ma J, et al. The role of N-linked glycosylation in protein folding, membrane targeting, and substrate binding of human organic anion transporter hOAT4. Mol Pharmacol. 2005;67:868–876.
65 Eraly SA, Hamilton BA, Nigam SK. Organic anion and cation transporters occur in pairs of similar and similarly expressed genes. Biochem Biophys Res Commun. 2003;300:333–342.
66 Li T, Walsh JR, Ghishan FK, Bai L. Molecular cloning and characterization of a human urate transporter (hURAT1) gene promoter. Biochim Biophys Acta. 2004;1681:53–58.
67 Popowski K, Eloranta JJ, Saborowski M, Fried M, Meier PJ, Kullak-Ublick GA. The human organic anion transporter 2 gene is transactivated by hepatocyte nuclear factor-4 alpha and suppressed by bile acids. Mol Pharmacol. 2005;67:1629–1638.
68 Ljubojevic M, Herak-Kramberger CM, Hagos Y, Bahn A, Endou H, Burckhardt G, et al. Rat renal cortical OAT1 and OAT3 exhibit gender differences determined by both androgen stimulation and estrogen inhibition. Am J Physiol Renal Physiol. 2004;287:F124–F138.
69 Buist SC, Cherrington NJ, Choudhuri S, Hartley DP, Klaassen CD. Gender-specific and developmental influences on the expression of rat organic anion transporters. J Pharmacol Exp Ther. 2002;301:145–151.
70 Kobayashi Y, Ohshiro N, Shibusawa A, Sasaki T, Tokuyama S, Sekine T, et al. Isolation, characterization and differential gene expression of multispecific organic anion transporter 2 in mice. Mol Pharmacol. 2002;62:7–14.
71 Kobayashi Y, Hirokawa N, Ohshiro N, Sekine T, Sasaki T, Tokuyama S, et al. Differential gene expression of organic anion transporters in male and female rats. Biochem Biophys Res Commun. 2002;290:482–487.
72 Hosoyamada M, Ichida K, Enomoto A, Hosoya T, Endou H. Function and localization of urate transporter 1 in mouse kidney. J Am Soc Nephrol. 2004;15:261–268.
73 Pavlova A, Sakurai H, Leclercq B, Beier DR, Yu AS, Nigam SK. Developmentally regulated expression of organic ion transporters NKT (OAT1), OCT1, NLT (OAT2), and Roct. Am J Physiol Renal Physiol. 2000;278:F635–F643.
74 Nakajima N, Sekine T, Cha SH, Tojo A, Hosoyamada M, Kanai Y, et al. Developmental changes in multispecific organic anion transporter 1 expression in the rat kidney. Kidney Int. 2000;57: 1608–1616.
75 Enomoto A, Takeda M, Tojo A, Sekine T, Cha SH, Khamdang S, et al. Role of organic anion transporters in the tubular transport of indoxyl sulfate and the induction of its nephrotoxicity. J Am Soc Nephrol. 2002;13:1711–1720.
76 Deguchi T, Kusuhara H, Takadate A, Endou H, Otagiri M, Sugiyama Y. Characterization of uremic toxin transport by organic anion transporters in the kidney. Kidney Int. 2004;65: 162–174.
77 Villar SR, Brandoni A, Anzai N, Endou H, Torres AM. Altered expression of rat renal cortical OAT1 and OAT3 in response to bilateral ureteral obstruction. Kidney Int. 2005;68:2704–2713.
78 Quaglia NB, Brandoni A, Ferri A, Torres AM. Early manifestation of nephropathy in rats with arterial calcinosis. Ren Fail. 2003;25:355–366.
79 Sakurai Y, Motohashi H, Ogasawara K, Terada T, Masuda S, Katsura T, et al. Pharmacokinetic significance of renal OAT3 (SLC22A8) for anionic drug elimination in patients with mesangial proliferative glomerulonephritis. Pharm Res. 2005; 22:2016–2022.
80 Brandoni A, Villar SR, Picena JC, Anzai N, Endou H, Torres AM. Expression of rat renal cortical OAT1 and OAT3 in response to acute biliary obstruction. Hepatology. 2006;43: 1092–1100.
81 Sauvant C, Holzinger H, Gekle M. Prostaglandin E2 Inhibits Its Own Renal Transport by Downregulation of Organic Anion Transporters rOAT1 and rOAT3. J Am Soc Nephrol. 2006; 17:46–53.
82 Wolff NA, Grunwald B, Friedrich B, Lang F, Godehardt S, Burckhardt G. Cationic amino acids involved in dicarboxylate binding of the flounder renal organic anion transporter. J Am Soc Nephrol. 2001;12:2012–2018.
83 Feng B, Dresser MJ, Shu Y, Johns SJ, Giacomini KM. Arginine 454 and lysine 370 are essential for the anion specificity of the organic anion transporter, rOAT3. Biochemistry. 2001;40:5511–5520.
84 Hong M, Zhou F, You G. Critical amino acid residues in transmembrane domain 1 of the human organic anion transporter hOAT1. J Biol Chem. 2004;279:31478–31482.
85 Tanaka K, Zhou F, Kuze K, You G. Cysteine residues in the organic anion transporter mOAT1. Biochem J. 2004;380:283–287.
86 Hong M, Xu W, Yoshida T, Tanaka K, Wolff DJ, Zhou F, et al. Human organic anion transporter hOAT1 forms homooligomers. J Biol Chem. 2005;280:32285–32290.
87 Zhou F, Pan Z, Ma J, You G. Mutational analysis of histidine residues in human organic anion transporter 4 (hOAT4). Biochem J. 2004;384:87–92.
88 Zhou F, Tanaka K, Pan Z, Ma J, You G. The role of glycine residues in the function of human organic anion transporter 4. Mol Pharmacol. 2004;65:1141–1147.
89 Eraly SA, Vallon V, Vaughn DA, Gangoiti JA, Richter K, Nagle M, et al. Decreased renal organic anion secretion and plasma accumulation of endogenous organic anions in OAT1 knock-out mice. J Biol Chem. 2006;281:5072–5083.
90 Sykes D, Sweet DH, Lowes S, Nigam SK, Pritchard JB, Miller DS. Organic anion transport in choroid plexus from wild-type and organic anion transporter 3 (Slc22a8)-null mice. Am J Physiol Renal Physiol. 2004;286:F972–F978.
91 Takeda M, Khamdang S, Narikawa S, Kimura H, Hosoyamada M, Cha SH, et al. Characterization of methotrexate transport and its drug interactions with human organic anion transporters. J Pharmacol Exp Ther. 2002;302:666–671.
92 Nozaki N, Kusuhara H, Endou H, Sugiyama Y. Quantitative evaluation of the drug – drug interactions between methotrexate and nonsteroidal anti-inflammatory drugs in the renal uptake

process based on the contribution of organic anion transporters and reduced folate carrier. J Pharmacol Exp Ther. 2004;309: 226–234.

93 Shitara Y, Sato H, Sugiyama Y. Evaluation of drug-drug interaction in the hepatobiliary and renal transport of drugs. Annu Rev Pharmacol Toxicol. 2005;45:689–723.

94 Ishikawa T, Tsuji A, Inui K, Sai Y, Anzai N, Wada M, et al. The genetic polymorphism of drug transporters: functional analysis approaches. Pharmacogenomics. 2004;5:67–99.

95 Fujita T, Brown C, Carlson EJ, Taylor T, de la Cruz M, Johns SJ, et al. Functional analysis of polymorphisms in the organic anion transporter, SLC22A6 (OAT1). Pharmacogenet Genomics. 2005;15:201–209.

96 Bleasby K, Hall LA, Perry JL, Mohrenweiser HW, Pritchard JB. Functional consequences of single nucleotide polymorphisms in the human organic anion transporter hOAT1 (SLC22A6). J Pharmacol Exp Ther. 2005;314:923–931.

97 Anzai N, Jutabha P, Kanai Y, Endou H. Integrated physiology of proximal tubular organic anion transport. Curr Opin Nephrol Hypertens. 2005;14:472–479.

98 Anzai N, Miyazaki H, Noshiro R, Khamdang S, Chairoungdua A, Shin HJ, et al. The multivalent PDZ domain-containing protein PDZK1 regulates transport activity of renal urate-anion exchanger URAT1 via its C-terminal. J Biol Chem. 2004;279: 45942–45950.

99 Miyazaki H, Anzai N, Ekaratanawong S, Sakata T, Shin HJ, Jutabha P, et al. Modulation of renal apical organic anion transporter 4 function by two PDZ domain-containing proteins. J Am Soc Nephrol. 2005;16:3498–3506.

100 Jiang W, Prokopenko O, Wong L, Inouye M, Mirochnitchenko O. IRIP, a new ischemia/reperfusion-inducible protein that participates in the regulation of transporter activity. Mol Cell Biol. 2005;25:6496–6508.

101 Okamoto T, Schlegel A, Scherer PE, Lisanti MP. Caveolins, a family of scaffolding proteins for organizing "preassembled signaling complexes" at the plasma membrane. J Biol Chem. 1998;273:5419–5422.

102 Kwak JO, Kim HW, Oh KJ, Kim DS, Han KO, Cha SH. Co-localization and interaction of organic anion transporter 1 with caveolin-2 in rat kidney. Exp Mol Med. 2005;37:204–212.

103 Kwak JO, Kim HW, Song JH, Kim MJ, Park HS, Hyun DK, et al. Evidence for rat organic anion transporter 3 association with caveolin-1 in rat kidney. IUBMB Life. 2005;57:109–117.

104 He W, Miao FJ, Lin DC, Schwandner RT, Wang Z, Gao J, et al. Citric acid cycle intermediates as ligands for orphan G-protein-coupled receptors. Nature. 2004;429:188–193.

105 Markovich D, Murer H. The SLC13 gene family of sodium sulphate/carboxylate cotransporters. Pflugers Arch. 2004;447: 594–602.

106 Asif AR, Steffgen J, Metten M, Grunewald RW, Muller GA, Bahn A, et al. Presence of organic anion transporters 3 (OAT3) and 4 (OAT4) in human adrenocortical cells. Pflugers Arch. 2005;450:88–95.

Available online at www.sciencedirect.com
SCIENCE DIRECT
Toxicology and Applied Pharmacology 210 (2006) 200–211
Toxicology and Applied Pharmacology
www.elsevier.com/locate/ytaap

Prenatal 3,3′,4,4′,5-pentachlorobiphenyl exposure modulates induction of rat hepatic CYP 1A1, 1B1, and AhR by 7,12-dimethylbenz[*a*]anthracene

Shin Wakui[a,*], Kiyofumi Yokoo[a], Hiroyuki Takahashi[b], Tomoko Muto[c], Yoshihiko Suzuki[d], Yoshikatsu Kanai[c], Hiroshi Hano[b], Masakuni Furusato[e], Hitoshi Endou[c]

[a]*Department of Toxicologic Pathology, Azabu University School of Veterinary Medicine, 1-17-71 Fuchinobe, Kanagawa 229-8501, Japan*
[b]*Department of Pathology, The Jikei University School of Medicine, Tokyo 105-8461, Japan*
[c]*Department of Pharmacology and Toxicology, Kyorin University School of Medicine, Tokyo 181-8611, Japan*
[d]*Department of Biochemistry, Azabu University School of Veterinary Medicine, Kanagawa 229-8501, Japan*
[e]*Department of Pathology, Kyorin University School of Medicine, Tokyo 181-8611, Japan*

Received 8 February 2005; accepted 30 April 2005
Available online 28 June 2005

Abstract

We previously reported the finding that prenatal exposure to a relatively low dose of PCB126 increases the rate of DMBA-induced rat mammary carcinoma, while a high dose decreased it. One of the most important factors determining the sensitivity to mammary carcinogenesis is the metabolic stage at administration of the carcinogenic agent. DMBA is a procarcinogen that recruits the host metabolism to yield its ultimate carcinogenic form, and CYP1A1 and CYP1B1 (CYP1) conduct this metabolism. We investigated the hepatic expression of CYP1 and AhR following oral administration of DMBA (100 mg/kg b.w.) (i.g.) to 50-day-old female Sprague–Dawley rats whose dams had been treated (i.g.) with 2.5 ng, 250 ng, 7.5 μg of PCB126/kg or the vehicle on days 13 to 19 post-conception. Real-time quantitative RT-PCR analysis revealed that the prenatal exposure to a relatively low dose of PCB126 (the 250 ng group) prolonged the higher expression of CYP1A1, CYP1B1, and AhR mRNA, while prenatal exposure to a high dose of PCB126 (the 7.5 μg group) prolonged the higher expression of CYP1A1 and AhR mRNA. Western blotting and immunohistochemical analyses were consistent with mRNAs changes. Because DMBA oxidation produces a highly mutagenic metabolite and is finally catalyzed by CYP1B1, a relatively low PCB126 dose might produce the biological character to potentially increase the risk of DMBA-induced mammary carcinoma.

Keywords: PCB126; DMBA; CYP1; AhR; Liver; Rat

Introduction

Polychlorinated biphenyls (PCBs) are a heterogeneous group of man-made organic compounds that are widely present in the environment (IARC, 1997). The chemical stability and lipophilicity of PCBs and their resistance to degradation results in their persistence and concentration in food chains (Bro-Rasmussen, 1996) as well as their bioaccumulation in human adipose tissue (Kutz et al., 1991), blood (Murphy and Harvey, 1985), and breast milk (Rogan et al., 1987). Moreover, transplacental and lactational transfers of PCBs to a developing fetus and infant have the potential to cause adverse effects (Safe and Krishnan, 1995; van den Berg et al., 1998).

7,12-Dimethylbenz[*a*]anthracene (DMBA) is a model compound that induces mammary carcinogenesis in rodents (Huggins et al., 1961; MacDonald et al., 2001; Rowlands et

Abbreviations: PCBs, polychlorinated biphenyls; CYP, cytochrome P450; AhR, aryl hydrocarbon receptor; ARNT, AhR nuclear translocator protein; PCB126, 3,3′,4,4′,5-pentachlorobiphenyl; DMBA, 7,12-dimethylbenz[*a*]anthracene.

* Corresponding author. Fax: +81 42 754 7661.
E-mail address: wakui@azabu-u.ac.jp (S. Wakui).

0041-008X/$ - see front matter © 2005 Elsevier Inc. All rights reserved.
doi:10.1016/j.taap.2005.04.022

al., 2001). We previously found that prenatal exposure to a relatively low dose of 3,3′,4,4′,5-pentachlorobiphenyl (PCB126) increases rat mammary carcinoma induced by DMBA ingestion at 50 days old, and exposure to a high dose of PCB126 acts as an inhibiting agent for it (Muto et al., 2001). One of the most important factors determining sensitivity to mammary carcinogenesis is the metabolic stage of the carcinogenic agent. DMBA is a procarcinogen and requires metabolic conversion to its ultimate carcinogenic metabolite by oxidation, which is conducted by CYP1A1 and 1B1 (CYP1) (Christou et al., 1987; Dipple, 1995; Shimada et al., 1996). Both the proximate and ultimate metabolites of DMBA that are formed in hepatocytes can be transported to other organs, resulting in carcinogen-adducted DNA (Di Giovanni and Juchau, 1980; Ginsberg and Atherholt, 1989). Therefore, the liver has a primary role in the metabolism of DMBA and is the most significantly affected organ following the experimental exposure of DMBA to an animal (Di Giovanni and Juchau, 1980; Kothari and Subramanian, 1992). Thus, the extent to which DNA adducts occur after administration of DMBA depends on the level of oxidative metabolism of DMBA due to CYP1 activities (Dipple et al., 1999; Granberg et al., 2000; MacDonald et al., 2001; Rowlands et al., 2001).

Both PCB126, a prototypical coplanar halogenated aromatic hydrocarbon, and DMBA, a polycyclic aromatic hydrocarbon, bind and activate the aryl hydrocarbon receptor (AhR), which is a basic helix–loop–helix (b-HLH) protein (Burback et al., 1992). Ligand binding results in activation of AhR and subsequent nuclear translocation, where it heterodimerizes with another bHLH partner, the AhR nuclear translocator protein (ARNT) (Hoffman et al., 1991). The AhR–ARNT dimer binds to specific regulatory elements, xenobiotic responsive elements (XREs), upstream of the responsive genes and enhances their transcripts, the CYP1 enzyme family (Dolwick et al., 1993; Jones et al., 1986; Okey et al., 1994; Rowlands et al., 2001; Schmidt and Bradfield, 1996). Enzyme activation of carcinogens yields intermediate metabolites that are chemically more reactive than the initial compound (Cavalieri et al., 2002). Hence, we investigated the expressions of hepatic CYP1 and AhR following ingestion of DMBA by 50-day-old offspring of female rats that had been exposed to PCB126 on days 13 to 19 post-conception.

Materials and methods

Animals, chemicals, and treatments. Forty-five female and nine male 6-week-old Sprague–Dawley (slc) rats (Japan SLC, Shizuoka, Japan) were housed, three per plastic cage, on hardwood-chip bedding in an environment-controlled room on a 12-h light/12-h dark cycle at 22 ± 2 °C and 55% ± 5% relative humidity, with a conventional diet (MF, Oriental Yeast, Tokyo, Japan). All experimental procedures were conducted following approval of the Animal Care and Use Committee of the Azabu University School of Veterinary Medicine. Guidelines set by the National Institute of Health and Public Health Service Policy on the Humane Use and Care of Laboratory Animals were followed at all times. PCB126 was obtained from AccuStandard Inc., New Haven, CT, and DMBA was obtained from Tokyo Chemical Industry Co. Ltd., Tokyo, Japan. Seven-week-old rats were housed with five females and a male per plastic cage.

A lifetime tolerable daily intake (TDI) of PCB126 has been reported to range from 10 to 100 pg/kg/day (van den Berg et al., 1998). In this study, three doses of PCB126 were selected using 25 pg/kg/day as the TDI dose (Muto et al., 2001): 10^2-fold of the TDI dose, 10^4-fold of the TDI dose, and 3×10^5-fold of the TDI dose. Groups of eight pregnant rats were treated with 2.5 ng, 250 ng, or 7.5 μg/kg body (i.g.) PCB126 or with an equivalent volume of corn oil (~0.5 ml/animal, i.g.), on days 13 through 19 post-conception. The offspring were sexed at birth, and litters were reduced so that each dam was left with eight offspring (four females/dam). Weaning was carried out at day 21 post-partum. In this study, we considered the group of rats with prenatal exposure to 2.5 ng, 250 ng, or 7.5 μg/kg body PCB126 or with an equivalent volume of corn oil as the 2.5-ng, the 250-ng, the 7.5-μg, or the vehicle group, respectively.

Each PCB126-treated group (2.5-ng, 250-ng, or 7.5-μg group) included forty-five females, and the vehicle group included thirty-six females. For experiments, 135 fifty-day-old female rats received 100 mg/kg DMBA in corn oil/kg body (i.g.), and 36 received an equivalent volume of corn oil (~0.5 ml/animal, i.g.). In this study, the dose of DMBA was selected following the study of Huggins et al. (1961) with the conversion using animal body weight. Following anesthesia by diethyl ether, liver samples were obtained under deep anesthesia from five (DMBA-fed) and four (corn oil-fed) rats from each group at 6 h, 12 h, 1 day, 2 days, 5 days, 10 days, 20 days, and 30 days. Representative sections of each liver were fixed in 10% phosphate-buffered formalin and routinely processed for immunohistochemistry. In addition, representative sections were frozen without fixation and stored at −80 °C.

Chemical analysis. Analysis for PCB126 was carried out following the alkaline alcohol digestion method (Tanabe et al., 1987). Aliquots of homogenized rat mammary tumor samples were refluxed in 1 N KOH–ethanol solution for 1 h. The PCB126 thus extracted into ethanol was transferred to 100 ml of hexane by shaking in a separating funnel. Subsequently, the hexane layer was concentrated and purified by passing it through 1.5 g of silica gel (Wako gel S-1, Wako Co., Ltd., Osaka, Japan) packed in a glass column (10 mm inside diameter × 200 mm length). PCB126 was eluted with 200 ml of hexane at an elution rate of one drop per second. The eluate was concentrated to 5 ml in a Kuderna–Danish concentrator and further purified with 5% fuming sulphuric acid. All samples were injected into a gas chromatograph-mass spectrometer (GC-MS: Shimadzu 9020

DF with an SCAP-1123 data system, Shimadzu Co. Ltd., Kyoto, Japan) equipped with an electron-impact ion-source and moving needle-type injection system for the determination and identification of PCB126. The column consisted of a 0.23 mm I.D. × 30 m glass capillary, coated with silicone. Operating conditions of the GC-MS were as follows: column oven temperature was programmed to rise from 190 °C to 250 °C at 0.5 °C min^{-1}; injector and ion-source temperatures were kept at 250 °C and 280 °C, respectively. PCB126 was determined by selected ion monitoring at *m/z* 326. The carrier flow of helium was controlled at 0.6 ml min^{-1}.

Immunohistochemistry. Immunohistochemical expressions of CYP1A1 and CYP1B1 were analyzed using the avidin–biotin complex (ABC) method. After deparaffinization, 4 μm thick sections were treated sequentially with 0.3% H_2O_2 for 10 min, then blocked with 10% goat serum or horse serum in PBS for 20 min. Sections were thawed, rinsed in PBS, and treated with primary antibodies of rabbit anti-rat-CYP1A1 (Affiniti Res. Inc., Exeter, UK; diluted 1:1000) and rabbit anti-CYP1B1 (BD Biosciences, Bedford, MA; diluted 1:50). Bound IgG was detected with biotinylated goat anti-rabbit IgG (Vector Lab., Burlingame, CA; diluted 1:100) followed by avidin–biotin complex (ABC)-peroxidase (Vector Lab., Burlingame, CA) and diaminobenzidine (Sigma, St. Louis, MO). Sections were then counterstained with hematoxylin. As a negative control, non-immunized rabbit serum was substituted for the primary antibody.

Real-time quantitative RT-PCR. For each RNA sample, 100 ng was used as the template for first strand cDNA synthesis using a TaqMan Reverse Transcription kit, following the RT-PCR manufacturer's two-step protocol (PE Applied Biosystems, Foster City, CA). Controls included for each reaction were the RNA sample without reverse transcriptase (RNA − RT) and no RNA with reverse transcriptase (no RNA + RT). The conditions of the final reaction for reverse-transcription were as follows: 1 × TaqMan RT buffer; 5.5 mM $MgCl_2$; 500 μM dATP, dGTP, and dCTP; 1 mM dTTP; Random Hexamers 0.25 μM; 1.25 Ul MuLV reverse transcriptase and 0.4 U RNase inhibitor (PE Applied Biosystems, Foster City, CA). Quantitative analyses of target gene (CYP1A1, CYP1B1, and AhR) mRNA expression were performed by real-time quantitative PCR using the ABI Prism 7700 Sequence Detection System (PE Biosystems, Foster City, CA) with Taq Man chemistry and probe. The TaqMan probes and primers for target genes were assay-on-demand gene expression products (PE Applied Biosystems, Foster City, CA) and oligonucleotides with fluorescent reporter and quencher dyes attached (Table 1). Optimal primer, probe, and cDNA concentrations were determined in a separate set of experiments to insure that both target gene and GAPDH fragments were amplified with equal efficiency. PCR reactions were performed with first-strand cDNA synthesis (2 μl) from each sample, a Universal PCR Master Mix kit (PE Applied Biosystems, Foster City, CA), 250 nM TaqMan probe, 0.16 U of AmpErase UNG (uracil N-glycosylase), and 900 nM forward-reverse primers of the target gene and GAPDH. Three measurements per sample were performed in each of two independent experiments. Results were analyzed with the ABI Sequence Detector software version 1.7 (PE Applied Biosystems, Foster City, CA). For relative quantification of target gene expression, the standard curve method was applied. The calibrated standard curve of each target gene cDNA and GAPDH amplification plots were examined at five different dilutions (containing 100, 50, 25, 10, or 5 ng) of total RNA samples that were obtained from each PCR product using a TOPO II TA Cloning Kit (Invitrogen, Carlsbad, CA) following the manufacturer's recommendations. The target gene's normalized value was determined by dividing the average target gene value by the average GAPDH value. The standard deviation (SD) of the quotient is calculated from the SD of the target gene and GAPDH using the following formula:

$$CV = (\text{SD of the quotient})/(\text{mean value of the quotient})$$

$$(CV)^2 = (CV_1)^2 + (CV_2)^2$$

$$CV_1 = (\text{SD of target gene value})/(\text{mean of target gene value})$$

$$CV_2 = (\text{SD of GAPDH value})/(\text{mean of GAPDH value})$$

The normalized target gene value is a unitless number that can be used to compare the relative amount of the target gene in different samples. One way to make this comparison is to designate one of the samples as a calibrator. In this study, the liver of 50-day-old rat of the vehicle group without DMBA ingestion was designated as the calibrator, and the averaged target gene value was divided by the average calibrator value according to the manufacturer's instructions for quantification of relative gene expression (User Bulletin #2; P/N 4303859, pp. 3–30, 36).

Western blot analysis. Rat livers were homogenized in 50 mM Tris–HCl, 150 mM KCl (pH 7.4), 1% Triton X-100, and 0.25 mM phenylmethylsulfonyl fluoride (PMSF) and centrifuged at 8000 × *g* for 30 min at 4 °C. The supernatant obtained was centrifuged at 100,000 × *g* for 90 min at 4 °C.

Table 1
ID numbers of TaqMan probes and primers (Assay-on-Demand gene expression products) used for real-time quantitative RT-PCR

Gene	ID
CYP1A1	Rn0048721...ml
CYP1B1	Rn00564055...ml
AhR	Rn00565750...ml

Assay-on-Demand gene expression products were supplied by PE Applied Biosystems, Foster City, CA.

Table 2
Body and liver weights of 50-day-old female rats after prenatal PCB126 exposure

Group	Body weight (mg)	Liver weight (mg)
7.5 μg	242.25 ± 4.07	12.06 ± 0.89
250 ng	245.32 ± 4.21	12.22 ± 0.53
2.5 ng	243.26 ± 5.82	11.70 ± 0.55
Vehicle	243.22 ± 6.22	11.86 ± 0.76

Values represent mean ± SEM Scheffé's F test, NS.

The pellet was suspended in 50 mM Tris–HCl (pH 7.4), 1% Triton X-100, and 1 mM PMSF, and the protein concentrations were determined with a bicinchonic acid protein assay reagent kit (Pierce, Rockford, IL) with bovine serum albumin as a standard. Microsomal samples were subjected to electrophoresis on a 10% SDS polyacrylamide gel using 10 μg of microsomes. The proteins were transferred for 2 h to a nitrocellulose membrane that was blocked by immersing it in 5% non-fat dried milk in phosphate-buffered saline with 0.1% (v/v) Tween 20 (PBS-T). Western blot analysis was performed using anti-rat-CYP1A1 (Affiniti Res., Exeter, UK), anti-rat-CYP1B1 (BD Gentest, San Jose, CA), or anti-AhR (H-211) (Santa Cruz, Santa Cruz, CA) antibodies. CYP1A1, CYP1B1, and AhR antibodies were diluted 1:1000, 1:500, and 1:1000, respectively, in PBS-T and incubated 1 h at room temperature on an orbital shaker. After being washed three times with PBS-T, they were incubated with a 1:2500 dilution of horseradish peroxidase-conjugated anti-rabbit antibody (Amersham Biosciences, Piscataway, NJ) for 1 h on an orbital shaker. After being washed three times with PBS-T, the membranes were detected using the ECL Plus Western Blotting Detection System (Amersham Biosciences, Piscataway, NJ).

Statistical analysis. For each set, the mean value, standard deviation, and standard error of the mean were calculated and compared using Scheffé's F test or a chi-square test using the computer statistical analysis system Stat View-J 5.0 (Abacus Concepts, Cary, NC).

Results

Body and liver weights, and concentration of PCB126 in liver

Prenatal PCB126 treatment of dams resulted in offspring with body weights and liver weights that were similar between groups at 50 days old (Table 2). The concentration of PCB126 in the liver of 50-day-old rats compared to the vehicle group was about 365 times higher in the 7.5-μg group, about 12 times higher in the 250 ng group, and about 1.5 times higher in the 2.5 ng group, and that of 80-day-old rats compared to the vehicle group was about 26 times higher in the 7.5-μg group, about 1.4 times higher in the 250-ng group, and about 1.1 times higher in the 2.5-ng group (Table 3).

Table 3
Concentration of PCB126 in livers of female rats after prenatal exposure

Group	50-day-old	80-day-old
7.5 μg	73.05 ± 8.68*	5.01 ± 3.79
250 ng	2.35 ± 1.39	0.26 ± 0.96
2.5 ng	0.30 ± 0.98	0.21 ± 0.88
Vehicle	0.20 ± 0.42	0.19 ± 0.37

Values represent mean ± SEM ng/g.
* Scheffé's F test, $P < 0.05$.

Quantitative RT-PCR for CYP1A1 and CYP1B1 mRNA expression in prenatally PCB126-exposed rat liver

In 50-day-old rats, the 7.5-μg group showed significantly increased expression of hepatic CYP1A1 mRNA (33-fold) and CYP1B1 mRNA (15-fold), and the other groups showed lower expression of CYP1A1 mRNA (1- to 3-fold) and CYP1B1 mRNA (1- to 1.7-fold) (Figs. 1, 2). As they grew older, the CYP1 mRNA expression levels of the 7.5-μg group gradually decreased, but remained at significantly higher levels compared with that of the other groups until they were 70 days old (Figs. 1, 2).

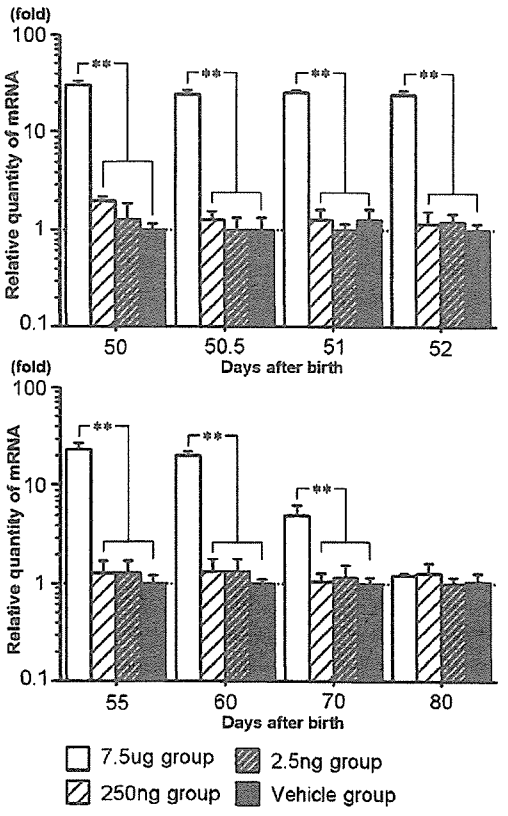

Fig. 1. Effect of prenatal exposure to PCB126 on CYP1A1 mRNA expression in rat liver. The indicated mRNA levels were determined by real-time quantitative RT-PCR, with analysis using the standard curve method described under Materials and methods. Each level was normalized to that of the endogenous housekeeping gene GAPDH in each tissue, as described under Materials and methods. Values represent mean ± SD. (**) Scheffé's F test $P < 0.01$.

Quantitative RT-PCR for CYP1A1mRNA expression following DMBA ingestion in prenatally PCB126-exposed rat liver

At 6 h after DMBA ingestion, the expression of CYP1A1 mRNA was significantly higher in all PCB126-treated groups (33- to 34-fold) than in the vehicle group (25-fold) (Fig. 3). After 12 h, all groups showed a similarly high level (Fig. 3). After 1 day, CYP1A1 mRNA expression of all PCB126-treated groups remained at high levels, but that of the vehicle group decreased to 25-fold (Fig. 3). After 2 days, CYP1A1 mRNA expression of the 7.5-μg and 250-ng groups remained at similarly high levels, but that of the 2.5 ng and vehicle groups decreased to 15- to 17-fold (Fig. 3). At 5 days after, CYP1A1 mRNA expression of the 7.5-μg and 250-ng groups showed a 28- to 32-fold increase, and that of 2.5-ng group had decreased 12-fold, while in the vehicle group, it had decreased to the calibrator level (Fig. 3). Subsequently, CYP1A1 mRNA expression of the 7.5-μg and 250-ng groups was gradually decreased to 22- to 28-fold at 10 days after, 18- to 20-fold at 20 days after, and CYP1A1 mRNA expression of the 2.5 ng and vehicle groups had returned to the calibrator level at 10 to 20 days after (Fig. 3). At 30 days after, CYP1A1 mRNA expression of all groups had returned to the calibrator level (Fig. 3).

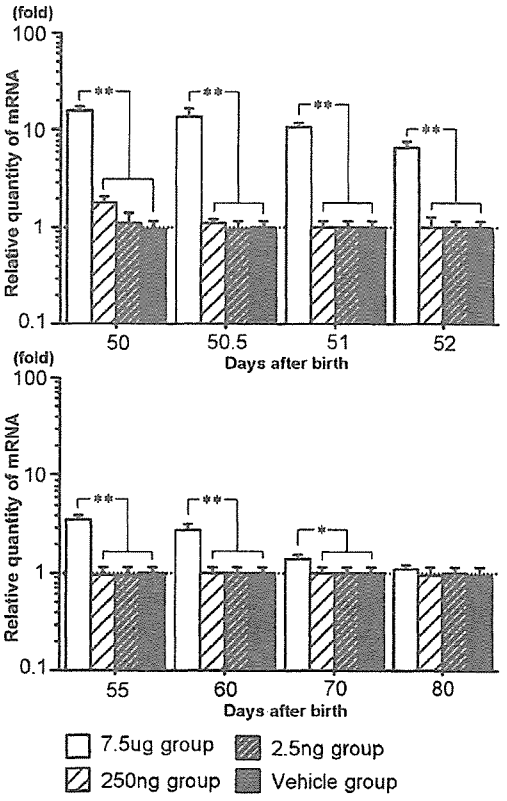

Fig. 2. Effect of prenatal exposure to PCB126 on CYP1B1 mRNA expression in rat liver. The indicated mRNA levels were determined by real-time quantitative RT-PCR, with analysis using the standard curve method described under Materials and methods. Each level was normalized to that of the endogenous housekeeping gene GAPDH in each tissue, as described under Materials and methods. Values represent mean ± SD. (**) Scheffé's F test $P < 0.01$. (*) Scheffé's F test $P < 0.05$.

Quantitative RT-PCR for CYP1B1mRNA expression following DMBA ingestion in prenatally PCB126-exposed rat liver

At 6 h after DMBA ingestion, the expression of CYP1B1 mRNA of all PCB126-treated groups had increased (24- to 26-fold), but that of the vehicle group remained at the calibrator level (Fig. 4). After 12 h to 1 day, CYP1B1 mRNA expression of the 7.5-μg and 250-ng groups increased further to 25- to 27-fold, and that of vehicle group also increased to 17- to 18-fold (Fig. 4). At 2 days after, CYP1B1 mRNA expression of the 7.5-μg and 250-ng groups remained at similarly high levels, but in the vehicle group it had decreased to 14-fold (Fig. 4). At 5 days after, CYP1B1 mRNA expression of the 250-ng group showed a 20-fold increase, which was significantly higher than that of the 7.5-μg and 2.5-ng groups (9- to 10-fold), and the vehicle group had decreased to the calibrator level (Fig. 4). After 10 to 20 days, CYP1B1 mRNA expression of the 250-ng group was 18-fold, which was significantly higher than that of the 7.5-μg group (8-fold), and the 2.5-ng and vehicle groups had returned to the calibrator level (Fig. 4). After 30 days, CYP1B1 mRNA expression of the 250-ng group was 2-fold, which was significantly higher than that of the 2.5-ng and vehicle groups (Fig. 4).

Quantitative RT-PCR for AhR mRNA expression following DMBA ingestion in prenatally PCB126-exposed rat liver

At 6 h after DMBA ingestion, the expression of AhR mRNA had increased, but those of all PCB126-treated groups (33-fold) were significantly higher than that of the vehicle group (25-fold) (Fig. 5). At 12 h after, AhR mRNA expression of all groups showed similarly high levels (Fig. 5). At 1–2 days after, AhR mRNA expression of the vehicle group gradually decreased (Fig. 5). At 5 days after, AhR mRNA expression of the 250-ng group was 35-fold, which was significantly higher than that of the 7.5-μg and 2.5-ng groups, and in the vehicle group, it had decreased to the calibrator level (Fig. 5). At 10–20 days after, AhR mRNA expression of the 250-ng group gradually decreased, but it was significantly higher than that of the 7.5-μg group, and in the 2.5-ng and vehicle groups, it was at the calibrator level (Fig. 5). After 30 days, all groups were at the calibrator level (Fig. 5).

Immunohistochemistry for CYP1A1 and CYP1B1, and Western blot analyses of CYP1A1, CYP1B1, and AhR expression following DMBA ingestion in prenatally PCB126-exposed rat liver

To determine whether the mRNA modulation of the CYP1 and AhR correlates with changes in protein expres-

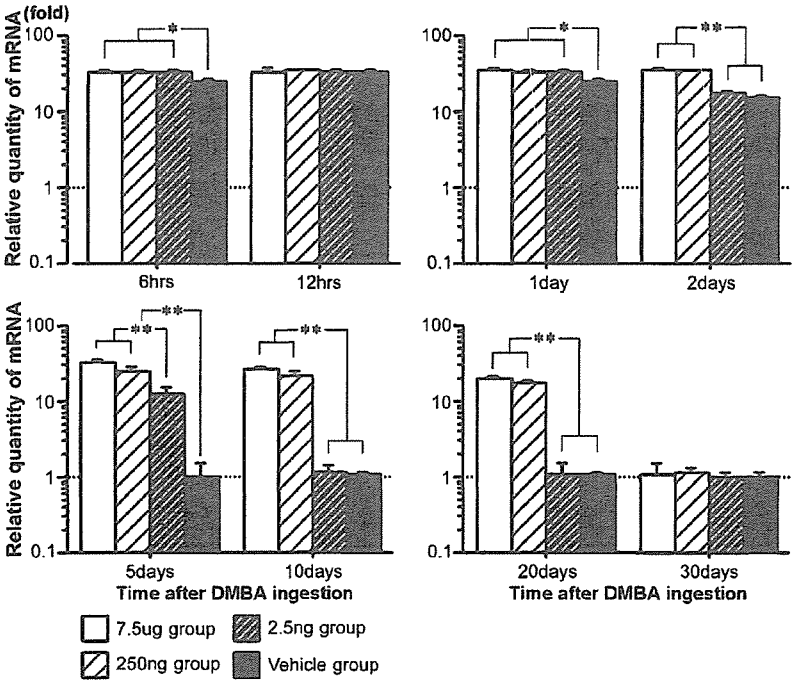

Fig. 3. Effect of prenatal exposure to PCB126 on CYP1A1 mRNA expression in rat liver following DMBA ingestion. The indicated mRNA levels were determined by real-time quantitative RT-PCR, with analysis using the standard curve method described under Materials and methods. Each level was normalized to that of the endogenous housekeeping gene GAPDH in each tissue, as described under Materials and methods. Values represent mean ± SD. (**) Scheffé's F test $P < 0.01$ (*) Scheffé's F test $P < 0.05$.

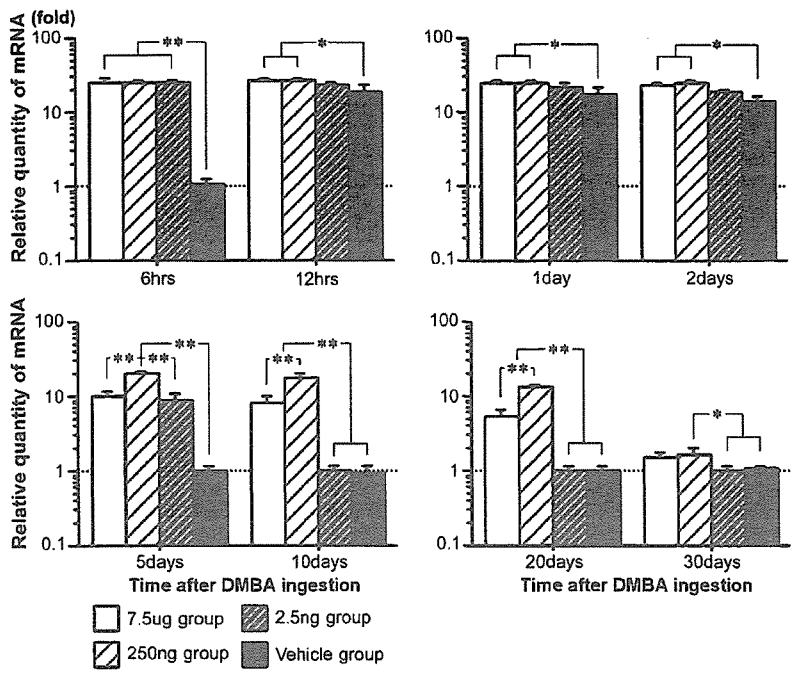

Fig. 4. Effect of prenatal exposure to PCB126 on CYP1B1 mRNA expression in rat liver following DMBA ingestion. The indicated mRNA levels were determined by real-time quantitative RT-PCR, with analysis using the standard curve method described under Materials and methods. Each level was normalized to that of the endogenous housekeeping gene GAPDH in each tissue, as described under Materials and methods. Values represent mean ± SD. (**) Scheffé's F test $P < 0.01$ (*) Scheffé's F test $P < 0.05$.

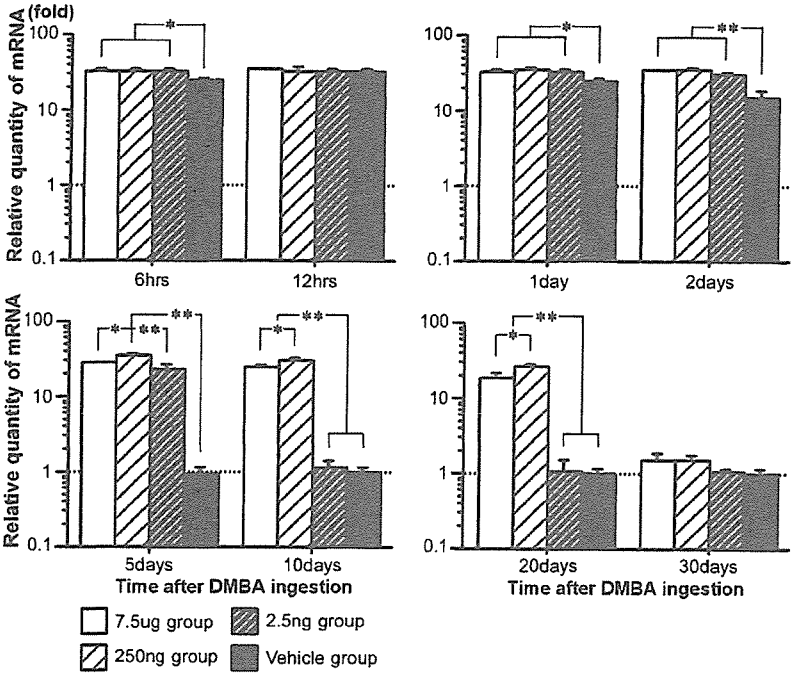

Fig. 5. Effect of prenatal exposure to PCB126 on AhR mRNA expression in rat liver following DMBA ingestion. The indicated mRNA levels were determined by real-time quantitative RT-PCR, with analysis using the standard curve method described under Materials and methods. Each level was normalized to that of the endogenous housekeeping gene control GAPDH in each tissue, as described under Materials and methods. Values represent mean ± SD. (**) Scheffé's F test $P < 0.01$ (*) Scheffé's F test $P < 0.05$.

sion, immunohistochemistry, and/or Western blot analyses were performed. The protein expression was qualitatively consistent with the patterns observed for CYP1A1 mRNA, CYP1B1 mRNA, and AhR mRNA (Figs. 6–8).

Discussion

PCBs are ubiquitous environmental contaminants that produce a spectrum of adverse biochemical and biological effects, including carcinogenic effects in people and a wide variety of animals (IARC, 1997). The induction of CYP1 expression by PCBs and DMBA has been extensively investigated (Angus et al., 1999; Christou et al., 1987; Rowlands et al., 2001; Schmidt and Bradfield, 1996; Whitlock, 1999), and it has been established that the nuclear AhR/ARNT heterodimeric complex acts as a ligand-activated transcription factor that binds to XREs in the regulatory region of CYP1 genes (Evans, 1988).

Our previous study found that rats given 250 ng PCB126/kg/day (from days 13 through 19 post-conception) had a higher incidence of DMBA-induced mammary carcinogenesis than a group given 7.5 μg PCB126/kg/day (from days 13 through 19 post-conception) (Muto et al., 2001). PCBs are considered non-genotoxic carcinogens because they do not produce DNA adducts and are negative for genotoxic tests (Turteltaub et al., 1990), while DMBA, a member of the polycyclic aromatic hydrocarbons (PAHs), is a procarcinogen and requires metabolic conversion to its ultimate carcinogen metabolite, DMBA-3,4-dihydrodiol-1,2-epoxide (Dipple et al., 1984; Slaga et al., 1979; Slims and Grover, 1981), by a process that includes two separate oxidations, produces 3,4-dihydrodiol, and is catalyzed by either CYP1A1 or CYP1B1 (Christou et al., 1987; Ciolino et al., 2002). The second oxidation produces the highly mutagenic 3,4-dihydrodiol-1,2-epoxide metabolite and is catalyzed by CYP1B1 (Shimada et al., 1996). These data suggest that CYP1B1 is an essential enzyme for metabolic activation, and thus the carcinogenic potential of DMBA is dependent on it. In this study, the 7.5-μg group showed higher expression of CYP1A1 until 20 days after DMBA ingestion, while the 250-ng group showed higher expression of CYP1A1 until 20 days after and higher expression of CYP1B1 until 30 days after. The mechanisms controlling the tissue-specific transcription of CYP1B1 are now not known (Sasaki et al., 2003). Our results are the first demonstration, to our knowledge, of a modulation of CYP1B1 expression by PAHs. Indeed, it has been suggested that CYP1B1 possesses a greater capacity than CYP1A1 to bioactivate a number of PAH procarcinogens (MacDonald et al., 2001; Shimada et al., 1996). Because Western blotting and immunohistochemical analyses were qualitatively consistent with each mRNA change, increased activities of these enzymes would also be revealed in the increased protein expression.

When DMBA was ingested at 50 days old, only the 7.5-μg group showed a high level of hepatic CYP1 expression, and it had decreased to that of the calibrator level at 80 days